เสถียรภาพของตัวเร่งปฏิกิริยาอะลูมินาเฟสผสมสำหรับปฏิกิริยาขจัดน้ำของเอทานอล

นางสาวจารุรัตน์ สัมพันธ์วณิช

วิทยานิพนธ์นี้เป็นส่วนหนึ่งของการศึกษาตามหลักสูตรปริญญาวิศวกรรมศาสตรมหาบัณฑิต
สาขาวิชาวิศวกรรมเคมี ภาควิชาวิศวกรรมเคมี
คณะวิศวกรรมศาสตร์ จุฬาลงกรณ์มหาวิทยาลัย
ปีการศึกษา 2557

STABILITY OF MIXED-PHASE ALUMINA CATALYSTS FOR ETHANOL DEHYDRATION REACTION

Miss Jarurat Sumphanwanich

A Thesis Submitted in Partial Fulfillment of the Requirements
for the Degree of Master of Engineering Program in Chemical Engineering
Department of Chemical Engineering
Faculty of Engineering
Chulalongkorn University
Academic Year 2014

Thesis Title	STABILITY OF MIXED-PHASE ALUMINA CATALYSTS FOR ETHANOL DEHYDRATION REACTION
By	Miss Jarurat Sumphanwanich
Field of Study	Chemical Engineering
Thesis Advisor	Associate Professor Bunjerd Jongsomjit, Ph.D.

Accepted by the Faculty of Engineering, Chulalongkorn University in Partial Fulfillment of the Requirements for the Master's Degree

.....Dean of the Faculty of Engineering
(Professor Bundhit Eua-arporn)

THESIS COMMITTEE

.....Chairman
(Associate Professor Seeroong Prichanont, Ph.D.)
.....Thesis Advisor
(Associate Professor Bunjerd Jongsomjit, Ph.D.)
.....Examiner
(Assistant Professor Kasidit Nootong, Ph.D)
.....External Examiner
(Doctor Ekrachan Chaichana, D.Eng.)

จารุรัตน์ สัมพันธ์วณิช : เสถียรภาพของตัวเร่งปฏิกิริยาอะลูมินาเฟสผสมสำหรับปฏิกิริยาขจัดน้ำของเอทานอล (STABILITY OF MIXED-PHASE ALUMINA CATALYSTS FOR ETHANOL DEHYDRATION REACTION) อ.ที่ปรึกษาวิทยานิพนธ์หลัก: รศ. บรรเจิด จงสมจิตร, หน้า.

ปฏิกิริยาการขจัดน้ำเป็นหนึ่งในเทคนิคที่สำคัญต่อการผลิตเอทิลีนจากเอทานอลโดยใช้อุณหภูมิที่ต่ำกว่าปฏิกิริยาไพโรไลซิสซึ่งถือว่าเป็นพลังงานทางเลือกที่สำคัญในอนาคต ในปัจจุบันมีการศึกษาและพัฒนาประสิทธิภาพของตัวเร่งปฏิกิริยาเพื่อให้ได้ตัวเร่งปฏิกิริยาที่มีประสิทธิภาพสูง โดยปัจจัยหลักที่ส่งผลต่อการเสื่อมสภาพของตัวเร่งปฏิกิริยาได้แก่ ค่าความเป็นกรดและอุณหภูมิ

จากงานวิจัยที่ผ่านมา พบว่าการเตรียมตัวเร่งปฏิกิริยาวัฏภาคผสมแกมมาและไคของอะลูมินาโดยวิธีทางโซลโวเทอร์มอล เผาที่อุณหภูมิ 600 องศาเซสเซียส และทดสอบความสามารถของตัวเร่งปฏิกิริยาด้วยปฏิกิริยาการขจัดน้ำของเอทานอลในวัฏภาคแก๊สที่ความดันบรรยากาศ อุณหภูมิระหว่าง 200 ถึง 400 องศาเซลเซียส ในเครื่องปฏิกรณ์แบบเบดคงที่ พบว่าช่วงระหว่างอุณหภูมิ 350 ถึง 400 องศาเซลเซียส ค่าการเปลี่ยน (conversion) ของเอทานอลและความสามารถในการเลือกเกิด (selectivity) ของเอทิลีนสูงมากกว่า 90% อย่างไรก็ตาม เสถียรของตัวเร่งปฏิกิริยาวัฏภาคผสมถูกศึกษาต่อในงานวิจัยนี้ที่อุณหภูมิคงที่ในช่วง 300 ถึง 400 องศาเซลเซียส เป็นเวลา 6 และ 12 ชั่วโมง ลักษณะของการเกิดโค้กจะปรากฏบนผิวของตัวเร่งปฏิกิริยาวัฏภาคผสมภายหลังการเกิดปฏิกิริยาการขจัดน้ำของเอทานอล จากการทดลองเมื่อเวลาผ่านไป 12 ชั่วโมง ปริมาณโค้กสะสมบนตัวเร่งปฏิกิริยาวัฏภาคผสมสูงขึ้นส่งผลทำให้ตัวเร่งปฏิกิริยาวัฏภาคผสมเสื่อมสภาพ ดังนั้นปัจจัย เช่นอุณหภูมิและเวลา ส่งผลกระทบต่อการเกิดการสะสมของโค้กอย่างมีนัยสำคัญ คุณลักษณะของตัวเร่งปฏิกิริยาวัฏภาคผสมก่อนและหลังใช้งานถูกเปรียบเทียบและอภิปรายต่อไป นอกจากนี้ การปรับปรุงตัวเร่งปฏิกิริยาวัฏภาคผสมด้วยโมลิบดินัมออกไซด์ถูกนำมาศึกษาภายใต้เงื่อนไขเดียวกันกับตัวเร่งปฏิกิริยาวัฏภาคผสมเพื่อเปรียบเทียบประสิทธิภาพและลักษณะของตัวเร่งปฏิกิริยาในการคาดการณ์จุดเหมาะสมของอุณหภูมิที่ใช้ในปฏิกิริยาการขจัดน้ำของเอทานอล

ภาควิชา วิศวกรรมเคมี ลายมือชื่อนิสิต .....

สาขาวิชา วิศวกรรมเคมี ลายมือชื่อ อ.ที่ปรึกษาหลัก .....

ปีการศึกษา 2557

5571014321 : MAJOR CHEMICAL ENGINEERING
KEYWORDS: DEACTIVATION, ETHANOL DEHYDRATION REACTION, MIXED-PHASE ALUMINA, OPTIMUM TEMPERATURE, STABILITY

JARURAT SUMPHANWANICH: STABILITY OF MIXED-PHASE ALUMINA CATALYSTS FOR ETHANOL DEHYDRATION REACTION. ADVISOR: ASSOC. PROF. BUNJERD JONGSOMJIT, Ph.D., pp.

Dehydration reaction is an important and basic technology for converting ethanol into ethylene product which temperature is less than pyrolysis reaction. It is also considered as alternative energy for future. Many researches improve and modify catalyst in order to obtain high selectivity. The selectivity factor mostly depends on acidity on a catalyst and temperature, which is catalytic early degradation.

In this present study, the mixed gamma and chi crystalline phases of alumina catalyst calcined at 600 °C was employed for ethanol dehydration to ethylene. The mixed γ- and χ-crystalline phase alumina was prepared by solvothermal method. The catalyst was performed for ethanol dehydration reaction under atmospheric pressure at temperature of 200-400 °C in a fixed-bed reactor. They exhibited both high conversion and high selectivity to ethylene more than 90% of interval temperature 350-400°C. The catalyst was characterized by several techniques. However, the stability of these catalysts will be further investigated by reaction test at the specified temperature (300-400°C) within time-on-stream (TOS) around 6 and 12 hrs.. The coke formation will appear on the surface of spent catalysts. After TOS 12 hrs., the coke content reaches very high level, which affects to catalyst deactivation. Therefore, the operating condition (such a TOS and temperature) leads to generate coke deposited on the catalysts significantly. The different characteristics of the fresh and spent catalysts will be compared and discussed further. Moreover, the modified MoO_3 loading on mixed γ- and χ-crystalline phase alumina catalysts were investigated catalytic performance at the same condition of TOS in order to study effective of metal oxide and compare with mixed phase alumina catalysts for predicable the optimum temperature.

Department:	Chemical Engineering	Student's Signature	.....
Field of Study:	Chemical Engineering	Advisor's Signature	.....
Academic Year:	2014		

ACKNOWLEDGEMENTS

I would like to express the deepest appreciation to my thesis advisor, Associate Professor Bunjerd Jongsomjit Ph.D., who has attitude and substance of a genius. He continually and convincingly conveyed invaluable lesson, advice and encouragement throughout the research. Without his guidance and persistent help this dissertation would not have been possible.

I am grateful to chairman committee, Assoc. Prof. Seeroong Prichanont, Ph.D., examining committee, Asst. Prof. Kasidit Nootong, Ph.D, and external examining committee, Dr. Ekrachan Chaichana, D.Eng., for spending time to review and those suggestions that contributed to improvement of my thesis.

I am sincerely thanks to chemical engineering lab at Chulalongkorn University for providing instrument for my research and Thai Nishi Institute (TNI) for giving me opportunity to present my dissertation in The 3rd National Interdisciplinary Academic Conference meeting.

Finally, I would like to express my deepest gratitude to my family and my friend for all they support throughout the period of research.

CONTENTS

Page

TABLES CONTENTS

FIGURES CONTENTS

CHAPTER I

INTRODUCTION

1.1 General introduction

Ethylene is an important preliminary product of petrochemical industry and many requirements in the world. This is because ethylene is mostly used in reactant for produced a variety of polymers such as polyethylene (PE), polypropylene (PP), polyvinyl chloride (PVC) and so on. Moreover, it is also employed as intermediate compounds of ethylene dichloride, ethylene oxide and ethyl benzene as well as fibres and other organic chemicals [1-3]. However, these products are launched on consumer markets such as the packaging, transportation, electrical/electronic, textile and construction industries as well as consumer chemicals, coatings and adhesives. Global ethylene production on 1 Jan. 2013 was more than 2 million tons larger than the capacity of last year as reported by Warren R. True [4]. **Tables 1.1-1.2** show the rankings of ethylene production complexes in the world.

Table 1.1 Top ten ethylene complexes of capacity rank (1 Jan. 2013)

No.	Company	Location	Capacity (tons/yr.)
1	Formosa Petrochemical Corp.	Mailian, Taiwan	2,935,000
2	Nova Chemical Corp.	Joffre, Alta	2,811,792
3	Arabian Petrochemical Co.	Jubail, Saudi Arabia	2,250,000
4	ExxonMobil Chemical Co.	Baytown, Tex.	2,197,000
5	ChevronPhillips Chemical Co.	Sweeny, Tex.	1,865,000
6	Dow Chemical Co.	Terneuzen, Netherlands	1,800,000
7	Ineos Olefins & Polymers	Chocolate Bayou, Tex.	1,752,000
8	Equistar Chemicals LP	Channelview, Tex.	1,750,000
9	Yanbu Petrochemical Co.	Yanbu, Saudi Arabia	1,705,000
10	Equate Petrochemical Co.	Shuaiba, Kuwait	1,650,000

Table 1.2 Regional capacity breakdown for ethylene

Region	Ethylene capacity, (tons/yr.)	
	1 Jan. 2013	**1 Jan. 2012**
Asia-Pacific	43,101,000	42,631,000
Eastern Europe	7,971,000	7,971,000
Middle East, Africa	26,007,000	24,557,000
North America	35,035,926	34,508,000
South America	6,383,500	6,383,500
Western Europe	24,904,000	24,904,000
Total capacity	143,402,426	140,954,500

Normally, ethylene is produced in the petrochemical industry by stream thermal cracking of hydrocarbon such as naphtha, liquefied petroleum gas and gas oil. The stream thermal cracking or pyrolysis method requires high thermal temperature around 750-900°C because of its endothermic reaction [5]. Nowadays, crude oil petroleum is concerned about non-renewable resource and limited consumer. Therefore, a new way to produce ethylene is being created from definition of "Green chemical process technologies". The classified of green process based on natural bioethanol, which is produced from fermentation of sugar cane or corncob, avoiding the use of food products. Ethylene is obtained by dehydrating bioethanol vapor using a catalyst containing a mixture of magnesium oxide, alumina, silica and etc. [6] that can reduce the thermal energy, cost and also friendly environment to enhance yield in chemical process development.

When demand for resource is in the high growth, the renewable biomass is the best choice to produce bioethanol and subsequently being converted into light olefins. It is an alternative approach to conventional stream thermal cracking in this time. Many researches are developed the ethanol dehydration reaction by using solid acid catalysts in order to generate ethylene faster and control reaction rate deliberately. Therefore, we have to consider the primary dehydration of ethanol to form ethylene and secondary etherification of ethanol to form diethyl ether. Both reactions require different temperatures, which can specify suitable operating condition. Zhang X. *et al.* (2008) [7] investigated catalyst capable of exhibiting high efficiency as well as stability in ethylene formation. The selectivity of four catalysts (Al_2O_3, HZSM-5, SAPO-34 and NiAPSO-34) was studied on suitable catalysts in order to find the activity and stability. The maximum selectivity of ethylene on HZSM-5 (98.5%) > NiAPSO-34 (98.3%) > SAPO-34 (94.3%) > Al_2O_3 (91.9%) at 300°C, 350°C, 350°C and 450°C, respectively. HZSM-5 exhibited greater activity

than other catalysts at lower temperature. Nevertheless, the stability of HZSM-5 was lowest among three remaining catalysts because of its strong acidic property. In contrast, NiAPSO-34 and SAPO-34 showed 92.3% and 86.0% yield of ethylene at time on stream (TOS) of 100 hrs. Therefore, NiAPSO-34 appeared to be better stability and activity than other catalysts. Bedia J. *et al.* (2011) [8] used acid carbon catalysts that were synthesized from olive stone with phosphoric acid (H_3PO_4). The catalytic decomposition of ethanol over the activated carbons can produce mainly dehydration of ethylene more than amount of diethyl ether in the activation temperature of 800°C with an impregnation ratio of 2. HA2-800 had the best results with around 95% selectivity of ethylene at 350 °C and TOS of ethanol conversion around 125 min before deactivation.

The main catalysts, which are used for ethanol dehydration reaction are based on γ-Al_2O_3 and HZSM-5 zeolite. Generally, the former required higher reaction temperature and lower product selectivity than zeolite. However, zeolite catalyst rapidly deactivated by coke formation. Therefore, researcher concentrates on alumina modification because γ-Al_2O_3 catalyst has excellent thermal stability, fine particle size, high surface area in adsorption and inhibits side reaction. Jenness G. R. *et al.* (2014) [9] examined the heterogeneity of the Al^{3+} binding sites for 100 and 110 facets of γ-Al_2O_3 by using the binding energy of a set of oxygenates. It was found that Al^{+3} site of the (110) surface exhibits the strongest Lewis acidity, which correlates with adsorption of binding energy.

The objective of this research is to study stability of mixed-phase alumina and modified metal oxide on mixed-phase alumina for optimal operating condition via ethanol dehydration reaction. The result is investigated physicochemical properties by using several techniques such as XRD, N_2 physisorption, NH_3 –TPD, TGA and SEM.

1.2 Research objectives

1.2.1 To investigate the stability of high conversion and high selectivity of the mixed gamma and chi crystalline phase catalysts and modified MoO_3-alumina catalysts in the specified temperature to find the optimum temperature for highly maintained ethylene selectivity.

1.2.2 To investigate characteristic of fresh and spent catalysts via time-on-stream (TOS) condition for ethanol dehydration reaction.

1.2.3 To explore the amount of coke on mixed-phases and modified alumina catalysts after reaction test for 6 and 12 hrs.

1.3 Research scopes

1.3.1 Preparation of gamma and chi crystalline phases catalysts in ratio (50 ml.) toluene and (50 ml.) 1-butanol via solvothermal method and calcined at 600°C.

1.3.2 Modification of 5wt% MoO_3 on mixed-phases of alumina catalysts by impregnation method

1.3.3 Verification of the characteristic of fresh catalysts for mixed phase alumina and 5wt% MoO_3 loading on mixed phase alumina by using X-ray diffraction (XRD), N_2 physisorption (BET) and NH_3-temperature programmed desorption (NH_3-TPD) technique.

1.3.4 Investigation the stability of catalysts in ethanol dehydration reaction within TOS around 6 and 12 hrs. under atmospheric pressure at temperature of 300°C, 350°C and 400 °C for mixed-phase and modified catalysts.

1.3.5 Investigation of the characteristic of spent catalysts after reaction at 6 and 12 hrs. via thermogravimetric analysis (TGA), scanning electron microscopy and energy X-ray spectroscopy (SEM-EDX) technique.

1.3.6 Comparison the selectivity of phase transition between pure gamma phase and mixed gamma-chi phase alumina catalysts.

1.4 Research methodology

Research methodology is shown as follows:

Part 1:

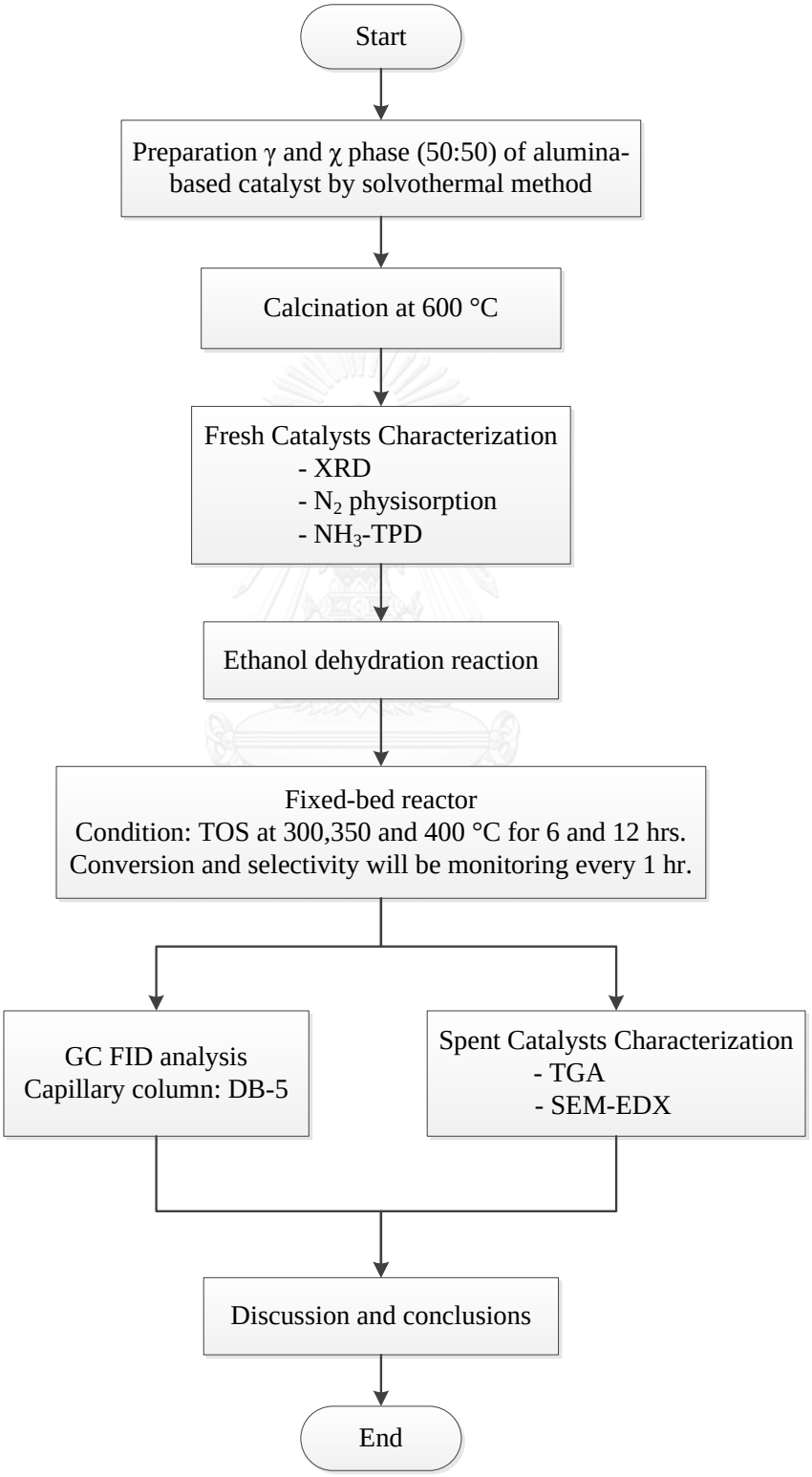

Part 2:

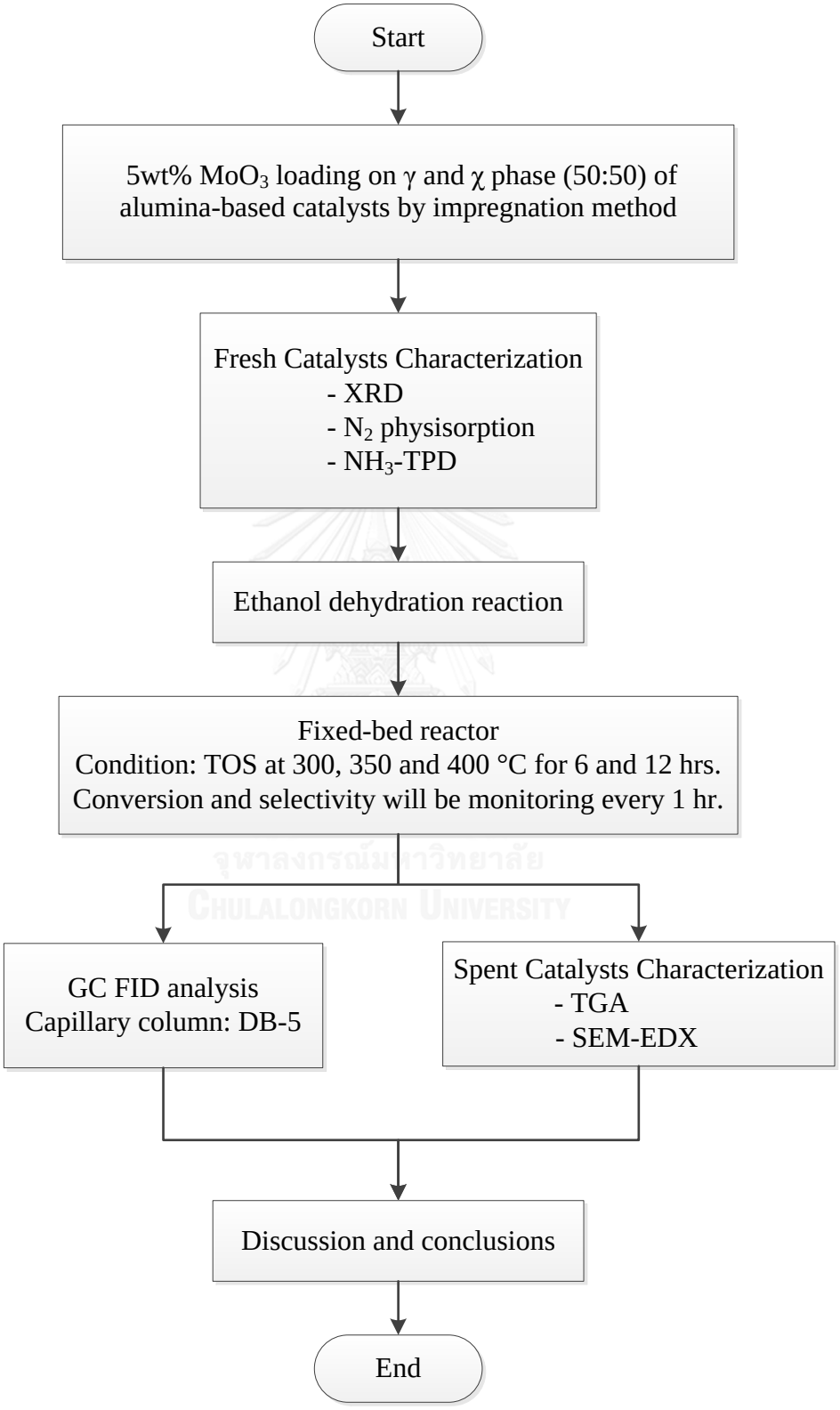

1.5 Research plan

Step	Works Description	2014-2015										
		Aug	Sep	Oct	Nov	Dec	Jan	Feb	Mar	Apr	May	Jun
1.	Literature Reviews.	←	—	—	→							
2.	Preparation of mixed-phase alumina catalysts and loading MoO_3 in of mixed-phase alumina catalysts			←	—	—	→					
3.	Fresh Characterization of mixed-phase alumina catalysts and loading MoO_3 in mixed-phase alumina catalysts			←	—	—	→					
4.	Perform the ethanol dehydration reaction						←	—	—	→		
5.	Spent Characterization of mixed-phase alumina catalysts and loading MoO_3 in mixed-phase alumina catalysts								←	→		
6.	Discussion and Conclusion										←	→

CHAPTER II
THEORY AND LITERATURE REVIEWS

The main ethylene process is produced from stream cracking of hydrocarbons using high energy consumption in reaction. At present, ethylene production still remains popular used in many chemical industries. Therefore, the catalytic dehydration reaction method will alternatively produce ethylene, which originates from bioethanol. The renewable knowledge sources are described in this chapter II below.

2.1 Ethanol dehydration reaction

The usual ethanol comprises hydroxyl group (-OH) in molecule, which occurs ethanol dehydration reaction in gas phase. Ethanol vapor is dehydrated by passing over heated acid catalysts to produce ethylene gas. This is collected over water and tested for typical properties of an unsaturated hydrocarbon. The dehydration reaction requires strong acid site or Brønsted acid site and also uses interval temperature around 180°C to 500°C [10-13]. Normal boiling point of ethanol and ethylene are 78.37°C and -103.7°C, respectively. Therefore, feed stream and product stream represent in gas phase. Two chemical competitive ways for ethanol dehydration reaction is represented by:

$$C_2H_5OH \rightarrow C_2H_4 + H_2O \qquad \Delta H^{298} = +44.9 \text{ kJ/mole} \qquad (1)$$

$$2C_2H_5OH \rightarrow C_2H_5O\,C_2H_5 + H_2O \qquad \Delta H^{298} = -25.1 \text{ kJ/mole} \qquad (2)$$

The first reaction is main reaction for dehydration of ethanol to ethylene that is endothermic, while the second one is side reaction for dehydration of ethanol to diethyl-ether (DEE) that is exothermic. Diethyl-ether is promoted at low temperature. On the other hand, dehydration reaction of main reaction favor at high temperature. Therefore, it concerns about activity of catalyst that can improve relatively reaction at low temperature in order to find a suitable catalyst for use in the industry. Especially, catalysts can be able to employ the hydrous ethanol. The ethanol dehydration mechanism is the E1 elimination reaction of alcohol. The E1 mechanism of alcohols can be described into 3 steps as follows:

Step1: Converting an alcohol to an alkene requires removal of the hydroxyl group. Protonation of the hydroxyl group allows it to leave as a water molecule. This step is very fast and reversible reaction. The lone pairs on the oxygen make it a Lewis base.

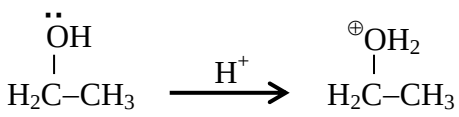

Step2: The species that remains has a carbon atom with only three bonds and a positive charge and is called a carbocation intermediate. The C-O bond allows the loss of neutral water molecule by using endothermic reaction. This step is the rate determining reaction because it occurs slowly.

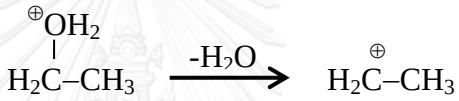

Step3: This intermediate species can be stabilized by loss of a proton from a carbon atom adjacent to the carbocation center leads to rearrange in which an alkyl group for creation of the alkene group (C=C) because carbocation intermedia are more stable (3° > 2° > 1°).

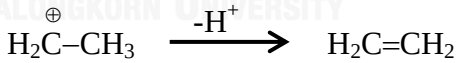

Therefore, overall of the E1 dehydration mechanism is shown as below.

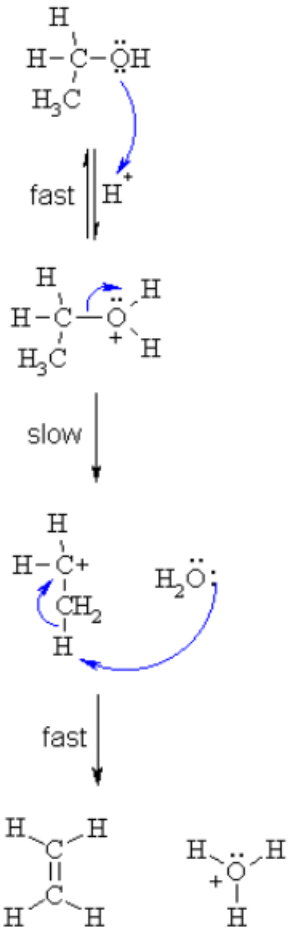

Figure 2.1 The mechanism of ethanol dehydration reaction to ethylene [14]

However, the formation of ethylene is also thermodynamically favored and requires high temperature above 100 °C. Operating a solid acid catalyst at temperature below 100 °C favors diethyl-ether in the selective formation but the kinetic reaction is limited and gives slow rate [15]. The bimolecular dehydration generates to form ether by substitution nucleophilic bimolecular reaction (S_N2). The mechanism of ethanol to diethyl-ether can be described into 3 steps and is shown in **Figure 2.2**.

Step1: The protonation from acid catalyst adds into alcoholic oxygen, which makes a better leaving group. This step is very fast and reversible reaction. The lone pairs on the oxygen make it a Lewis base.

Step2: The other alcoholic oxygen is nucleophile function, which attacks to electrophilic electron. The C-O bond allows the loss of neutral water molecule and creates an oxonium ion intermediate.

Step3: The protonated ether is removed proton (H^+) by molecule of water and rearranges to give the diethyl ether production.

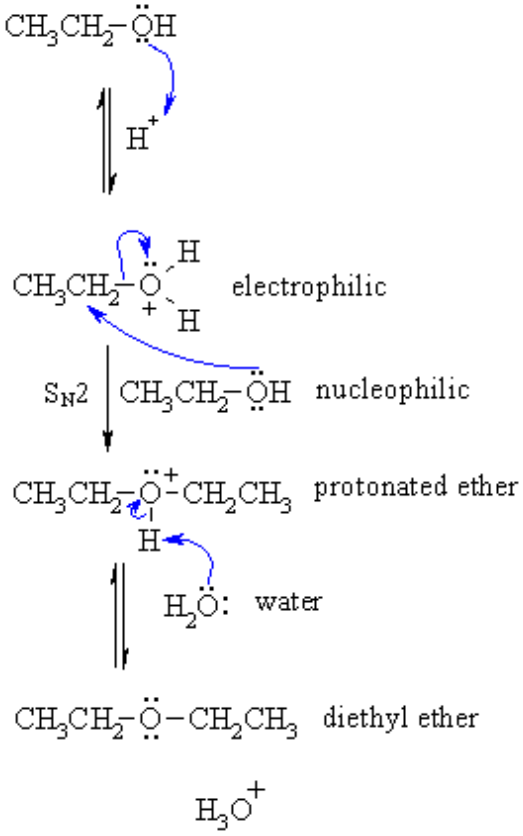

Figure 2.2 The mechanism of ethanol dehydration reaction to diethyl ether in S_N2 [16]

2.2 Catalyst

A heterogeneous catalyst is different phase from reactants and products. It is often favored in the industry because it easily separates the product after finished reaction. The heterogeneous catalysts are solid materials with the capability of adsorbing molecules of gases or liquids onto their surfaces, often a metal, a metal oxide or a zeolite [17]. After reaction, the products desorb from the surfaces and diffuse away.

However, catalysis has a much wider scope of application in chemical industry such as prevention of unwanted byproduct, transformation of reactant to easily product form and so on. Normally, the reactions can control on the basis of temperature, pressure, concentration and contact time [18]. The increase of temperature and pressure affect stoichiometric reactions into proceed rate of production. However, in the design plant, the limited condition is a thermodynamic under which product can be formed. Therefore, catalysis plays an important role, which can adjust processes to be carried out under industrially feasible condition of suitable temperature and pressure in order to save cost and energy and also obtain high efficiency of product.

2.2.1 Alumina oxide

This is the most famous catalyst in the process industry. The chemical formula of alumina oxide is Al_2O_3. The property of Al_2O_3 is the oxygen compound of aluminum with molar mass (M) = 101.96 g/mol, density (ρ) = 3.97 g/cm^3, boiling point (T_b) = 2,980°C and melting point (T_m) = 2,015°C. The white crystalline powder is found lump of various mesh sizes in different applications. Corundum is the natural alpha-alumina (α- Al_2O_3) or in hydrated forms. When it is doped with Cr^{3+} or Ti ions, the mineral is called ruby and sapphire, respectively [19]. The α- Al_2O_3 crystal structure is trigonal and it has a pseudo-hexagonal oxygen sub-lattice, which it is the most stable oxide form as shown in **Figure 2.3**. The alumina transition phases consist of chi phase (χ-Al_2O_3), gamma phase (γ-Al_2O_3), eta phase (η-Al_2O_3), theta phase (θ-Al_2O_3), delta phase (δ-Al_2O_3), kappa phase (κ-Al_2O_3) and rho phase (ρ-Al_2O_3). They can be produced by heat treatment (dehydration method) of aluminum hydroxides or aluminum salts, which generate different phase forms. For instance, gamma-alumina (or activated alumina) formed by dehydration at 500°C to 880°C and chi-alumina formed by dehydration at 350°C to 490°C. However, all transition phases at low temperature can covert to alpha phase at high temperature (1400°C).

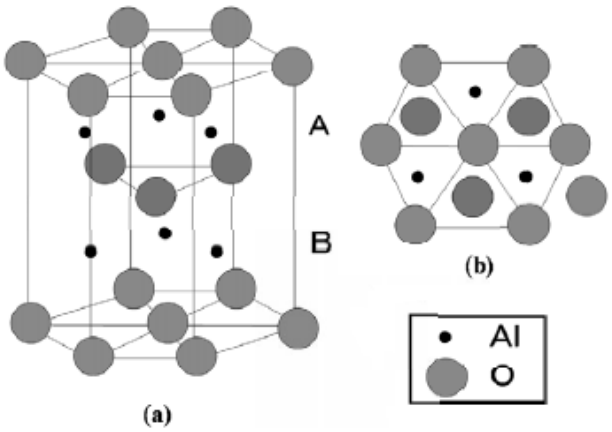

Figure 2.3 (a) Alpha phase of alumina structure and (b) top view of alpha-alumina structure [20]

Therefore, the structure transformation of aluminum oxide depends on calcination temperature as shown in **Figure 2.4**. Moreover, structural and compositional different forms of aluminum oxide are associated with particle size, surface area, surface reactivity and catalytic activity.

The formula reactants of aluminum oxide are shown as below.

- Bayerite (α-$Al(OH)_3$ or α-$Al_2O_3 \cdot 3H_2O$)
- Boehmite (γ-$AlO(OH)$ or γ-$Al_2O_3 \cdot H_2O$)
- Corundum (α-Al_2O_3)
- Diaspore (α-$AlO(OH)$ or α-$Al_2O_3 \cdot H_2O$)
- Gibbsite (γ-$Al(OH)_3$ or γ-$Al_2O_3 \cdot 3H_2O$)

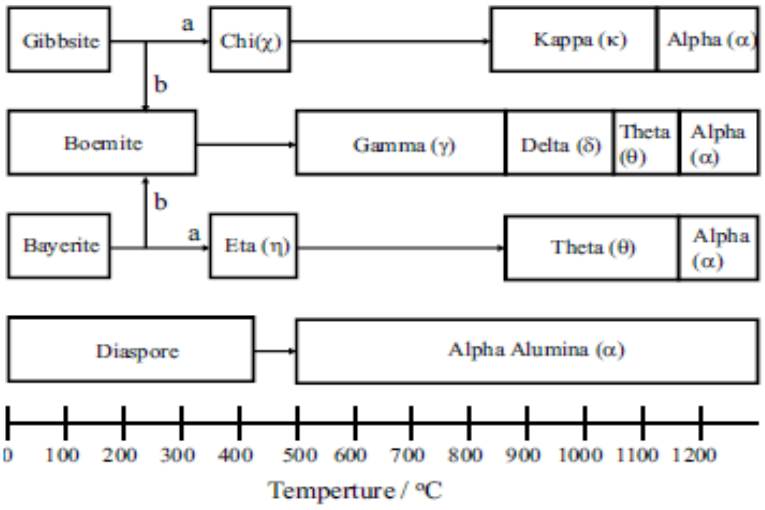

Figure 2.4 Thermal structural transformation of aluminum hydroxides [20]

In general, surface of aluminum oxide comprises of both acid site and basic site. The acid site is Lewis and Brønsted acid site on surface. Brønsted acid is a proton donor and Brønsted base is a proton acceptor. Lewis acid is an electron-pair acceptor and Lewis base is an electron-pair donor. A solid acid shows a tendency to donate a proton or to accept an electron pair, whereas a solid base tends to accept a proton or to donate an electron pair. However, the same site could serve as a Brønsted base as well as a Lewis base depending on the nature of the adsorbate in the reaction [21]. When water molecules in aluminum oxide are eliminated by calcination, it forms Lewis acid site and basic site as shown in **Figure 2.5** [22].

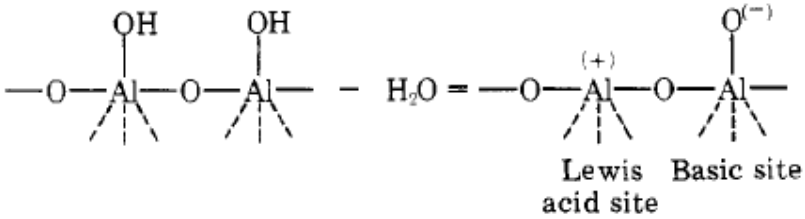

Figure 2.5 Lewis acid site and basic site formed on alumina

On the contrary, water molecules are added as pretreated catalyst, it transforms from Lewis acid site to weak Brønsted acid sites as shown in **Figure 2.6** [22].

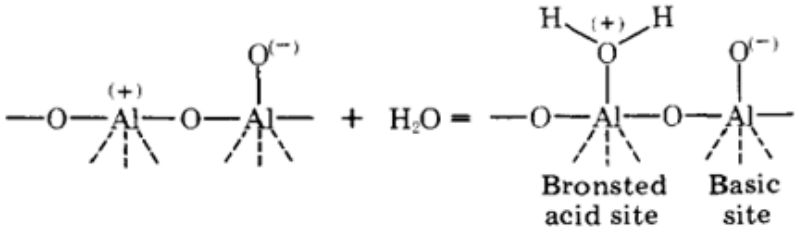

Figure 2.6 Brønsted acid sites formed on alumina

Aluminum oxides are widely used as adsorbents and catalysts in industrial process. For example, alpha-alumina is used as refractory material in furnace coating or laboratory equipment. Gamma-alumina is used as catalyst substrate or adsorptive agent. Moreover, aluminum oxide has established a worldwide position because of its advantages such as high corrosion resistance, light weight, readily fabricated by all commercial processes (welding, brazing, soldering) and so on. Therefore, many industrials are interested in use of aluminum oxides to apply in the process.

2.2.2 Molybdenum trioxide

Molybdenum and its compounds (oxides, sulphides, carbides, nitrides, selenides, molybdates and molybdenum complexes) have a number of applications in alloys, catalysts, electrochromics, sensors, capacitors, batteries, solar cells and so on. Molybdenum trioxide is chemical compound with the formula MoO_3, which is usually used to support on an inorganic oxide support (such as TiO_2, SiO_2, Al_2O_3, ZrO_2 and so on) in order to improve catalytic activity and selectivity, life, and mechanical strength. The molybdenum trioxides express a good catalytic performance for selective oxidation of hydrocarbons, oxidative dehydrogenation of alkanes, metathesis of olefins and hydrodesulfurization. Alumina and silica supported Mo catalysts have been important technology in industry.

In the solid state, anhydrous MoO_3 is composed of layers of distorted MoO_6 octahedra in an orthorhombic crystal. The octahedra share edges and form chains which are cross-linked by oxygen atoms to form layers. The octahedra have one short molydenum-oxygen bond to a non-bridging oxygen. The structure of molybdenum trioxide is shown in **Figure 2.7**

Many researcher have been studied the physical and catalytic properties of the molybdenum. Solsona B. *et al.* (2006) [23] proposed molybdenum–vanadium supported on mesoporous alumina catalysts. It was found that Mo-V-catalyst is more ethylene selectivity than the pure V-catalyst and Mo-catalyst. The optimal (Mo10V5) composition is presented a high selectivity to ethylene of 76% at an ethane conversion of 30%. The Mo-V-catalyst also presented vanadium and molybdenum species with a low degree of aggregation. Therefore, the improved selectivity to ethylene obtained in Mo-V-catalyst has two factors that are presence of highly selective vanadium species, as isolated VO_4 units and the coverage of non-selective sites of the support by molybdenum oxide species. El-Sharkawy E. A. *et al.* (2007) [24] investigated the structural properties and the thermal stability of molybdenum oxide on zirconia surface. At least 10wt% MoO_3 loading, MoO_x species retard the transformation of the tetragonal zirconia phase to monoclinic one. Mo^{6+} did not substitute Zr^{4+} to form solid solution at low Mo content because the radius of Mo^{6+} (66 pm) was much smaller than the radius of Zr^{4+} (84 pm). While increase of MoO_3 greater than 15wt% promoted the crystallize of MoO_3 and $Zr(MoO_4)_2$, the formation of $Zr(MoO_4)_2$ recorded at 2θ of 23.09, 30.58 and 50.04 at the indicate of MoO_3 phase and tetragonal zirconia phase, which is involved the elevation of thermal treatment > 800°C led to the decomposition of $Zr(MoO_4)_2$ into MoO_3 and monoclinic zirconia. However, the role of MoO_3 mainly depends on Mo/Zr ratio and calcination temperatures.

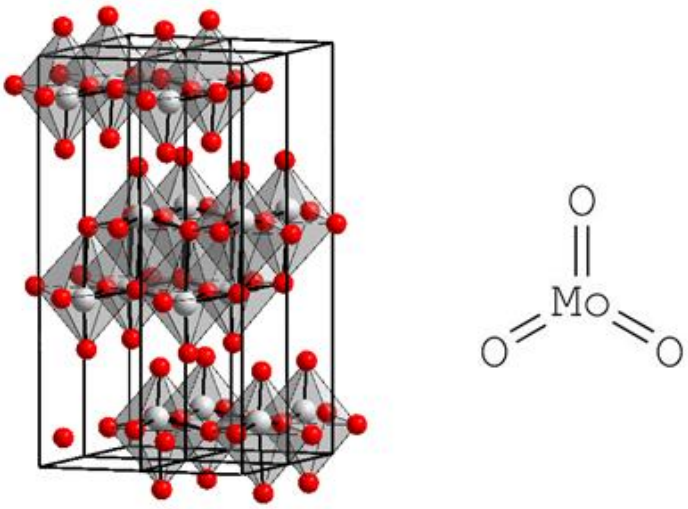

Figure 2.7 The molecular structure of molybdenum trioxide

2.2.3 Coke formation on catalyst (Deactivation of catalyst)

Coke formation is a type of physical fouling whereby the surface is covered with deposited carbon. During coke formation on catalyst, carbonaceous residues will form and cover the active surface sites of the catalyst, which can be illustrated in **Figure 2.8**.

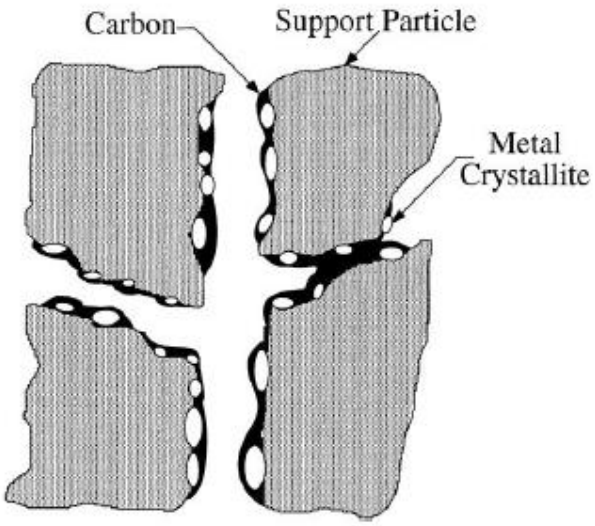

Figure 2.8 Coke formation on surface catalyst model [25]

When a layer or might be multilayers of chemisorbed carbon formed on the surface of catalyst active surface sites, it will block access the reactants to attach with the catalyst. It might also totally encapsulate the metal particle of catalyst thus, completely deactivate the catalyst. For the worst, the strong carbon filaments

that build-up in pores may stress and fracture the support material on catalyst caused disintegration of catalyst [25]. The decrease of active surface area will slowly deactivate the catalyst and cause decrease in the yield of product. For catalytic dehydration of bioethanol forming ethylene, the main cause of coke formation is due to the decomposition of ethylene forming carbon compound as shown in Equations 3 and 4.

$$C_2H_4 \leftrightarrow 2C + 2H_2 \quad (3)$$

$$C_2H_4 \leftrightarrow C + CH_4 \quad (4)$$

These are the two kinds of reaction that possibly occurs in decomposition of ethylene. The behavior of coke deposition is important to the kinetic study and reactor design. Wang, F., et al. (2011) [26] studied performance and coking behavior of submicron H-MFI catalyst for ethanol dehydration to ethylene. Average density becomes much bigger after the running because coke deposits were much condensed and unsaturated along the tube length, which may be attributed to a lower temperature and longer time on stream. The coke deposits take responsible for the acidity loss. Hu, H., et al. (2010) [27] described coke content as a function of reaction time (TOS). The dehydration of SAPO-34 during heating process has been observed by TGA instrument after methanol injection. The coke rate is higher due to reaction temperature rises and including concentration of adsorbed oligomers on the strong acid sites, which catalyst becomes the weight change and color interchanging phenomenon.

2.3 Solvothermal synthesis of aluminum oxide

The morphological synthesis of mesoporous aluminum oxide has many techniques such as calcination, precipitation, sol-gel, hydrothermal and solvothermal methods, which use different solvents for each reaction. Almost, the synthesis of aluminum oxide is usually performed by calcination of suitable precursors for remove the chemically combined water from the alumina hydrate, which requires the highly thermal energy for transformation. It affects the loss in the surface area and changes in surface properties [28]. The precipitation method is simple and inexpensive for Al_2O_3 synthesis, but the particles do not aggregate homogenous. It is leads to cause the low active dispersion [29, 30]. However, formation of Al_2O_3 can synthesize by using liquid-phase via sol-gel, hydrothermal and also solvothermal methods. These methods require temperature less than calcination method. The sol-gel route is formed from the both hydrolytic and non-hydrolytic method involving the use of metal alkoxides as starting materials or intermediates. Unfortunately, the stringent

experimental conditions are necessary for the hydrolysis of alkoxides and their relative higher cost [31].

The others hydrothermal and solvothermal synthesis are the best technique for morphological formation [32-36]. The general hydrothermal resembles the solvothermal method, but it differs in solvent. The definition of "hydro-" means water as solvent which "solvo-" means any kind of solvent such as alcohols, glycols, organic compound and so on. Nevertheless, the solvothermal method exhibits highly flexible and controllable easier hydrothermal method. It could be employed as an alternative to calcinations for the promotion of crystallization in organic media at moderate temperature (200-300°C) under autogenous pressure of the organics using an apparatus as shown in **Figure 2.9** The autogenous pressure is created by the vapor pressure of solvent. This is the minor effect on reaction rate. In other word, pressure does not affect reaction at temperature above or below the boiling point. Almost all controlled synthesis of nano- or micro particles concern two criterias; first criteria is crystallization growth in order to control size and shape particles and also second criteria is distribution monodispersed type in order to avoid effective or agglomeration. Therefore, the product synthesis via solvothermal method can be considered to prepare highly dispersed catalysts.

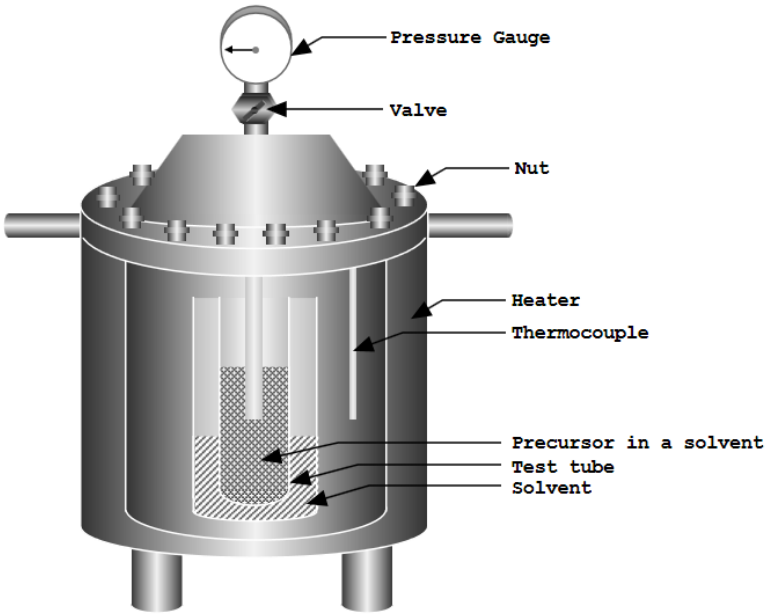

Figure 2.9 Apparatus for solvothermal reaction

2.4 Literature reviews

2.4.1 Ethanol dehydration reaction

Nowadays, the dehydration of ethanol has been interesting to produce ethane and diethyl ether (DEE) from non-petroleum feedstock. Many researchers have developed dehydration of ethanol, which is carried out in the gas phase on solid acid catalysts such as metal oxides, aluminas and zeolites [37]. Heterogeneous acid catalyst has attracted much interest in fundamental and applied research because it is benefit to economic and environmental.

Ramesh K. *et al.* (2009) [38] studied the influence of H_3PO_4 loading on the catalytic performance of modified H-ZSM-5 catalysts for the selective ethanol dehydration reaction. They discovered that surface area and pore volume of modified catalysts will significantly decrease when catalysts support is loaded at higher phosphoric acid contents. It affects to the formation of polymeric phosphates species at entrance of pore channels. The conversion of ethanol remains unchanged with 5%, 10% and 20% H_3PO_4 on ZSM-5 at 400°C but the selectivity of ethylene increase to above 98% on 20HP-ZSM-5 catalyst. However, H_3PO_4 modified catalysts have shown higher stability and deactivation after 110 hrs. when compared with unmodified HZSM-5 zeolite. In addition, the parent HZSM-5 catalyst has poor stability. The conversion of ethanol dehydration and selectivity to ethylene decreased with reaction time [39]. Bi J. *et al.* (2010) [40] found that the application of alumina catalysts for dehydration reaction is still important in industrial process, although it uses high thermal energy cost and low productivity. There are many reports on the selective production of ethylene from ethanol over microscale HZSM-5 zeolite catalyst. For example, Wu L.-P. *et al.* (2009) [17] reported the formation rate of ethylene over the TiO_2-supported zeolite composite catalyst was eight times higher than over ASZ (aluminosilicate zeolite) or TiO_2 at 420°C. While Xin H. *et al.* (2014) [41] treated by desilication with sodium hydroxide, dealumination with oxalic acid, or both of them, the result could display stable ethanol conversion and ethylene selectivity with time-on-stream around 12 hrs. for ZSM-deSi. However, the stability of microscale HZSM-5 zeolite catalyst is not satisfactory. Therefore, they developed HZSM-5 zeolite catalyst in nanoscale. The conversion of nano-CAT and the ethylene selectivity almost keep constant during 630 hrs., reaction at temperature 240°C; the conversion of bio-ethanol decreases from 99.20% to 98.40% while the selectivity of ethylene decreases from 98.69% to 98.43% from 420 hrs. to 630 hrs. of time-on-stream. For micro-CAT, the conversion of bio-ethanol decreases after 60 hrs. of TOS and lower than 95% after 140 hrs. The micro-CAT crystallize size is bigger than nano-CAT crystallize size. The former allows diffusion path longer than the latter over or inside

catalyst, which leads to the carbonaceous deposits. Therefore, the micro-CAT deactivated rapidly than nano-CAT.

Moreover, heterogeneous acid catalysis by heteropoly acids (HPAs) is the one choice for develop ethanol dehydration reaction. Bokade V. V. and G. D. Yadav (2011) [42] studied montmorillonite (K-10) and dodecatungestophosphoric acid (DTPA) supported on montmorillonite (DTPA/K-10), which was varied from 10 to 30% m/m. The 30% m/m DTPA/montmorillonite has shown the optimum dilute bio-ethanol conversion (74%), ethylene selectivity (92%) and diethyl ether selectivity (8%). The concentration of diethyl ether was found to decrease when increase DTPA loading from 10% to 30% of catalyst. The increase acidity with HPA loaded favors the activity and selectivity to ethylene. Another way of monitoring high conversions and selectivity depends on reaction temperature and space time when there are increasing. Varisli D. *et al.* (2007) [43] reported activities of three different HPAs that are silicotungstic acid (STA), molybdophosphoric acid (MPA) and tungstophosphoric acid (TPA). Among these three solid acid catalysts, STA showed the highest activity, but it does not mean highest acid strength in among of these.The acid strengths of TPA > STA > MPA follow reported by Wang Y. *et al.* (2000) [44]. The highest activity of STA was explained by the higher number of Keggin protons and the higher stability of STA than TPA at over temperature 200°C. However, the high ethylene yield (reaching to 0.77) was promoted by TPA at 250°C because of tungsten stronger acidity and higher thermal stability compared with molybdenum HPA [45].

2.4.2 Modification of Al_2O_3

Gamma alumina (γ-Al_2O_3) is a well-known in industrial solid catalyst because of its high surface area (50-300 m^2g^{-1}) and thermal stability up to 873 K [46]. Alcohols can dehydrate over γ-Al_2O_3 to form either olefins (ethylene) or ethers (DEE) via unimolecular or bimolecular, respectively. The γ-Al_2O_3 surface contains hydroxyl groups (-OH), which alumina (Al) atoms display Lewis acid sites and oxygen (O) atoms display Lewis base sites. The ethanol dehydration over γ-Al_2O_3 are likely to be Lewis acidic rather than Brønsted acidic. El-Katatny E. A. *et al.* (2000) [47] used aluminum dross tailings (ADT) and steel-pickling chemical waste (SPW) for the synthesis of alumina supported iron oxides (FeO_x/ Al_2O_3). Pure γ-Al_2O_3 support at 190-210°C is shown to maintain a higher selectivity of DEE (>90%), whereas the rising reaction temperature generate to ethene product. The DEE selectivity also depends on a function of W/F (W = catalyst weight and F = the total flow rate) because when W/F was increased, selectivity shifts to ethene. These mentions mean that ethanol dehydration to DEE is optimized under low temperature and low flow at atmospheric. Moreover, the loading of FeO_x species affect to increase ethylene formation. In the same way, Lewis acid sites (Al^{3+}) also support the formation of ethoxide ($C_2H_5O^- \rightarrow Al^{3+}$) surface species. Chen G. *et al.* (2007) [48] investigated

effects of TiO_2-doped on γ-Al_2O_3 catalysts. When TiO_2 deposited on alumina surface, it can affect the specific surface area (A_{BET}) and the pore volume (V_p). The surface area and the pore volume of TiO_2/γ-Al_2O_3 have a small size compared with pure Al_2O_3. They compared loading of 0wt%, 10wt% and 20wt% TiO_2 on γ-Al_2O_3. The results indicate that 10wt% TiO_2/γ-Al_2O_3 shows the strongest acidity while 20wt% TiO_2/γ-Al_2O_3 is exhibits the lowest acidity because TiO_2 dissociated from surface of Al_2O_3 and formed pure crystal phase. Therefore, the optimum loading of 10wt% TiO_2 can convert ethanol to ethylene nearly 100% at 460°C for high selectivity of ethylene as 98.7%, which is much higher than other ratios.

Recently, molybdenum species supported on different carrier have been proven to be effective in enhancing the dehydration reaction of low carbon alcohols. Han Y. *et al.* (2011) [49] promoted 5wt% Mo containing for effective detection of calcination on HZSM-5 in catalytic dehydration of ethanol. It was found that 5wt% Mo/HZSM-5 catalyst calcined at 500°C exhibited the highest weak and medium acidity, which it is better for stabilize performance in ethanol dehydration compared with parent HZSM-5. It is supposed that Mo species interacted and replaced the stronger Brønsted acid sites during the calcination procedure, but when continue rising calcined temperature, the acid sites decreased which could be explained by the dehydroxilation of Brønsted acid sites at high temperature or partially destruction of ZSM-5 zeolite. Bian G.-z. *et al.* (1998) [50] studied effect of samples with different Mo loading (5-45wt% MoO_3/ γ-Al_2O_3) for mixed alcohols synthesis from syngas. The results indicated two periods of Mo loading. First, 5-25wt% Mo loading showed the total yields of mixed alcohols and hydrocarbons decreased, but the selectivity to mixed alcohols was enhanced from 3% to 50%. In the second period, CO conversion was enhanced, but the selectivity to mixed alcohols decreased in 25-45wt%.

Besides, the improvement of acidic gamma alumina still involves synthesis of mixed phase alumina. Pansanga K. *et al.* (2008) [51] reported the synthesis of mixed phase between gamma and chi alumina under the solvothermal condition that can increase surface area and bulk density with increasing AIP concentration. As a result of morphology, it changes from a wrinkled sheet structure to small spherical particles. Furthermore, the mixed gamma and chi crystalline phases Al_2O_3 supported Co catalysts may prevent agglomeration of Co particles especially at high Co loading. It means higher dispersion of Co on the mixed phase Al_2O_3 supports as well as higher CO hydrogenation activities.

CHAPTER III
EXPERIMENTAL

This chapter describes laboratory procedures, step of catalytic preparation for mixed gamma and chi phases alumina including modified with molybdenum. Moreover, catalytic characterization and ethanol dehydration reaction are presented in this section below.

3.1 Catalytic preparation

The mixed gamma and chi crystalline phases of alumina were prepared via solvothermal method and were modified by impregnation method.

3.1.1 Chemicals

Table 3.1 The chemicals used for synthesis catalysts

Item	Chemical	**Supplier**
1	Aluminum isopropoxide : AIP (98%) $[(CH_3)_2CHO]_3Al$	Aldrich
2	Toluene (99%) $C_6H_5CH_3$	Merck
3	1-Butanol (99%) $C_4H_{10}O$	Merck
4	Methanol CH_3OH	Merck
5	Ultra high purity nitrogen gas (99.99%)	TIG
6	Ethanol C_2H_5OH (99.99%)	J.T.Baker
7	Ammonium heptamolybdate tetrahydrate $(NH_4)_6Mo_7O_{24}\cdot 4H_2O$	Merck

3.1.2 Synthesis of mixed-phase alumina catalysts

The mixed gamma and chi crystalline phase alumina catalysts were prepared via the solvothermal method. Aluminum isopropoxide (AIP) 25g was suspended in 100ml mixed solution (50ml toluene and 50ml 1-butanol) in a test tube. After that brought it in a 300ml autoclave, and then added 30ml solvent (15ml toluene and 15ml 1-butanol) in the gap between the test tube and the autoclave wall. The mixture is purged with nitrogen at pressure of 20 bar. The operating condition is heated up to 300°C at 2.5°C/min heating rate and holding for 2 hrs. After it was cooled down to room temperature, the resulting powder was washed with methanol several times by centrifugal machine at 20 rpm for 5 minutes and air drying overnight. The catalyst powder was calcined in a tube furnace for temperatures at 600°C with a heating rate of 10°C/min and holding in the air for 6 hrs.

3.1.3 Synthesis of Molybdenum trioxide (MoO_3) on mixed-phase alumina catalysts

The modification of 5wt% MoO_3 on mixed-phase alumina catalysts were prepared by impregnation method with an aqueous ammonium heptamolybdate tetrahydrate $(NH_4)_6Mo_7O_{24}\cdot 4H_2O$ solution. The procedure of modified catalyst preparation was calculated from 1g of catalyst used. First, ammonium heptamolybdate tetrahydrate was dissolved in deionized water (DI), and then dropped that solution into 1g of solid support. It was dried in the air at room temperature for 24 hrs., dried in oven at 110°C for 6 hrs. and calcined in the air at 500°C for 2 hrs.

3.2 Catalytic characterization

3.2.1 X-ray diffraction (XRD)

The bulk crystal structure and X-ray diffraction (XRD) patterns of the catalysts were determined by the SIEMENS D5000 X-ray diffractometer connected with a personal computer with Diffract ZT version 3.3 programs for fully control of the XRD analyzer. The experiment were carried out by using Cu K_α radiation source with Ni filter in the 2θ range of 20 to 80° with a resolution of 0.02°.

3.2.2 Nitrogen physisorption

The BET surface area, pore volume and pore diameter of catalysts were determined by nitrogen gas adsorption at liquid nitrogen temperature (-196°C) using Micromeritics ChemiSorb 2750 Pulse chemisorption System instrument. Before characterization, the sample was thermally treated at 150°C for 1 hr.

3.2.3 Temperature programmed adsorption (NH_3-TPD)

The acid properties of catalysts were investigated by temperature programmed adsorption of ammonia (NH_3-TPD) equipment by using Micromeritics chemisorp 2750 Pulse Chemisorption System. In an experiment, a packed quartz wool and 0.1 g of catalyst were loaded in a quartz tube and pretreated at 500°C under helium flow for 1 hr. The sample was saturated with 15%NH_3/He. After saturation, the physisorbed ammonia was desorbed under helium gas flow about 30 min., and then the sample was heated from 40°C to 800°C at heating rate 10°C.min^{-1}. The amount of ammonia in effluent was measured via TCD signal as a function of temperature.

3.2.4 Thermal gravimetric analysis (TGA)

The spent mixed-phase alumina catalysts were subjected to the thermal gravimetric analysis (Diamond Thermogravimetric and Differential Analyzer, TA Instruments SDT Q600) to determine the carbon content in the samples, as well as their thermal behaviors in the range of 30°C to 1,000°C. The analysis was performed at heating rate of 10°C.min^{-1} in 100ml.min^{-1} flow of air.

3.2.5 Scanning electron microscopy and Energy X-ray Spectroscopy (SEM-EDX)

Scanning electron microscopy was observed the morphologies of catalysts after TGA checked by using JEOL JSM-35 CF model. The elemental dispersion over the catalysts surface was determined by energy X-ray spectroscopy (EDX), which it was performed on Link Isis Series 300 program.

3.3 Reaction study in dehydration of ethanol

Material, equipment, operating condition and procedure for the ethanol dehydration reaction of mixed-phase alumina and modified MoO_3 on mixed-phase alumina catalysts are described in this section below.

3.3.1 Chemicals and reagents

The chemicals and reagents are shown in Table 3.2 for the ethanol dehydration reaction.

Table 3.2 Chemicals and reagents for the ethanol dehydration reaction

Item	Chemicals and Reagents	Supplier
1	High purity grade hydrogen (99.99 %)	TIG
2	Ultra high purity nitrogen gas (99.99 %)	TIG
3	Argon (UHP Grade 99.999%)	TIG
4	Ethanol (99.99 %)	Merck

3.3.2 Instruments and apparatus

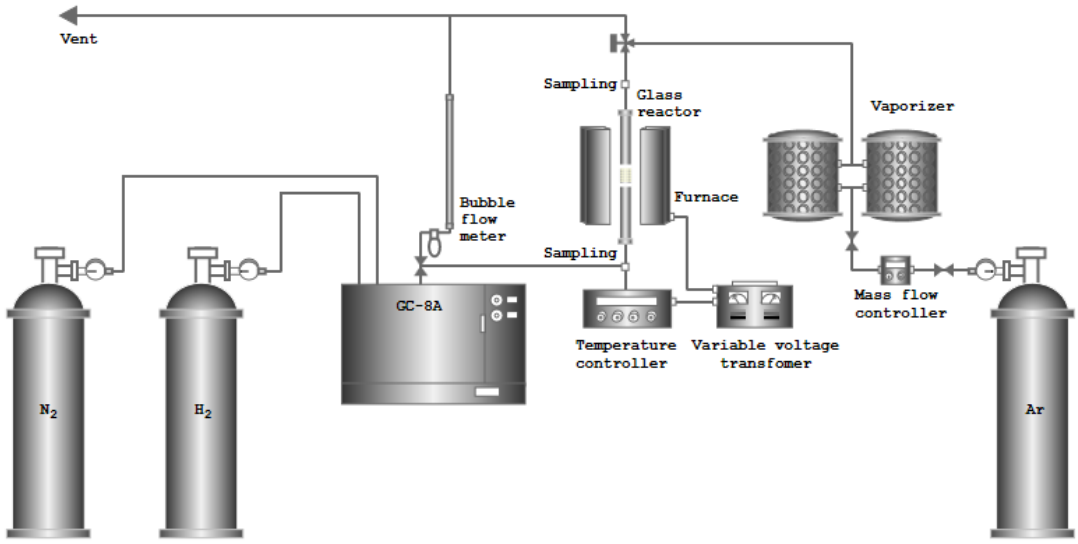

Figure 3.1 Ethanol dehydration reaction system

Diagram of ethanol dehydration reaction system is shown as follow **Figure 3.1**. All equipment in this diagram is described the principle of catalyst tests follow below.

- **Reactor**: The reactor tube has an inner diameter size 0.7 mm and length size 12 cm. It is made from borosilicate glass tube.
- **Vaporizer**: The vaporizer is stainless steel equipment that injecting ethanol in liquid phase is transformed to saturated vapor phase under atmospheric pressure by using syringe pump.
- **Electrical furnace and heating cable**: The reactor is supported by electrical furnace as heater. The temperature of electrical furnace is controlled via interoperability of variable voltage transformer and temperature controller at 190 Volt. The heating cable is enfolded on outlet reactor line in order to prevent the condensation of water dehydrated from reaction.
- **Temperature controller**: The temperature controller is connected with thermocouple attached to the reactor and a variable voltage transformer. In this research, the temperature is controlled set point via temperature controller at and 300°C, 350°C and 400°C for mixed phase alumina and Mo-modified on mixed-phase alumina catalysts.
- **Gas controlling system**: An inert gas (Argon) is used for carrier ethanol vapor into the reactor. The flow rate of carrier gas can adjust operating condition via on-off valve, mass flow controller and pressure regulator.

- **Gas chromatography machine (GC)**: The product stream was analyzed by Shimadzu gas chromatography with flame ionization detector (FID) via DB-5 capillary column. The operating condition which use in gas chromatography is shown in **Table 3.3** below.

Table 3.3 Operating condition for analytical product in gas chromatography

Item	Gas Chromatography Detail	Condition
1	**Detector**	FID
2	**Capillary column**	DB-5
3	**Carrier gas**	Nitrogen (99.99 vol.%)
		Hydrogen (99.99 vol.%)
4	**Column temperature**	
	- Initial	40°C
	- Final	40°C
5	**Injector temperature**	150°C
6	**Detector temperature**	150°C
7	**Time analysis**	12 min
8	**Analyzed gas**	Ethanol
		Ethylene
		Diethyl Ether
		Acetaldehyde

3.3.3 Catalyst tests in ethanol dehydration reaction

This experiment used 0.05 g. catalyst, which was packed in a continuous down-flow fixed-bed reactor with an inner diameter size 0.7 mm. at 200°C under ambient pressure. The catalyst was placed on 0.01 g. quartz wool in the middle of a borosilicate glass reactor. Previous in situ activation was performed under argon (60 $ml.min^{-1}$) at 200°C and 190 volt. The gas flow was kept during reaction, while absolute ethanol was fed into the reactor by using a syringe pump with a WHSV of 22.88 hr^{-1}. The temperature inside the reactor was controlled and measured by using a thermocouple located in the catalyst bed. The reaction was performed at temperature 300°C, 350°C and 400°C for mixed phase alumina and modified on mixed phase alumina catalysts.

Reaction products were continuously monitored by online gas chromatography using a Shimadu GC8A gas chromatography equipped with FID detector connected to DB-5 capillary column at 150°C every 1 hr. for 6 and 12 hrs.

CHAPTER IV
RESULTS AND DISCUSSION

This chapter explains verification of X-ray diffraction (XRD), nitrogen physisorption, temperature programmed adsorption (NH_3-TPD), thermal gravimetric analysis (TGA), scanning electron microscopy and energy X-ray spectroscopy (SEM-EDX) technique including catalyst tests in ethanol dehydration reaction. It consists of 3 parts in the chapter. Part1 describes characteristic and stability of mixed γ- and χ-crystalline phase alumina catalysts, part2 describes the modified metal oxide of MoO_3 loading on mixed γ- and χ-crystalline phase alumina catalysts and part3 compares catalysts of pure phase (G-Al), mixed phase (M-Al) and MoO_3 modification on mixed phase alumina (Mo-M-Al) for predicable catalytic performance in sections 4.1, 4.2 and 4.3, respectively.

4.1 Characteristic and stability of M-Al catalysts

4.1.1 Catalyst Characterization

4.1.1.1 X-ray diffraction (XRD)

Transitional alumina phase was characterized by using X-ray diffraction technique in order to prove and identify the structure of catalysts. XRD patterns of mixed-phase alumina catalysts synthesized via solvothermal method of AIP compound in 50:50 solution between toluene and 1-butanol were obtained. The catalysts were properly calcined at 600°C. The characteristic peaks of alumina reflect γ-phase at 2θ = 32°, 37°, 39°, 45°, 61° and 66° and χ-phase at 2θ = 37°, 40°, 43°, 46°, 60° and 67° confirms the transformation of mixed-phase [52]. **Figure 4.1** displays transition phase between G-Al phase and M-Al phase. The different M-Al phase peak can be detected having chi at 43°.

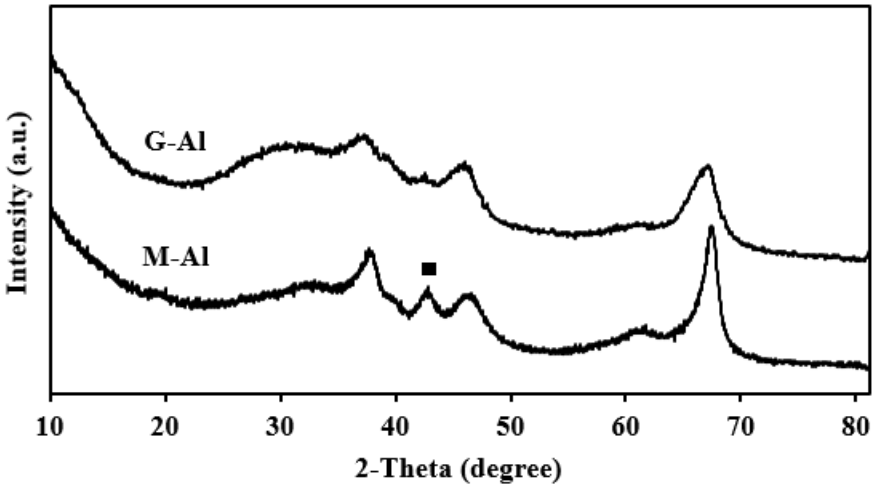

Figure 4.1 XRD patterns of G-Al phase and M-Al phase;
(■) chi-alumina phase at 43°

4.1.1.2 Nitrogen physisorption

The BET surface area of G-Al phase and M-Al phase samples were analyzed on the basis of nitrogen multilayer adsorption measured as a function of relative pressure using a fully automated analyzer to identify the total specific surface area in m^2/g unit. The BJH analysis can also be employed to find pore size and specific pore volume using adsorption-desorption isotherms as shown in **Figure 4.2**. It exhibited the IV-type isotherms follow IUPAC classification, indicating the existence of well-developed mesopores [53]. The pore diameter (D) is divided into three categories; macropores (D > 50 nm), mesopores (2 nm < D < 50 nm) and micropores (D < 2 nm) [54]. Therefore, the pore size distribution curve of the samples confirms to sort of unimodal with mesopores (2-28 nm) as shown in **Figure 4.3**. The pore structure parameters of the G-Al phase and M-Al phase samples are listed in **Table 4.1**. The phase transition did not influence to BET surface area, but it mix slightly affects the pore volume and the pore size diameter.

Table 4.1 BET surface area analysis and BJH pore size and volume analysis of G-Al phase and M-Al phase catalysts.

Sample	BET surface area	Pore volume	Pore size diameter
	S_{BET} (m^2/g)	P_V (cm^3/g)	P_d (nm)
M-Al	200	0.69	8.26
G-Al	201	0.64	8.55

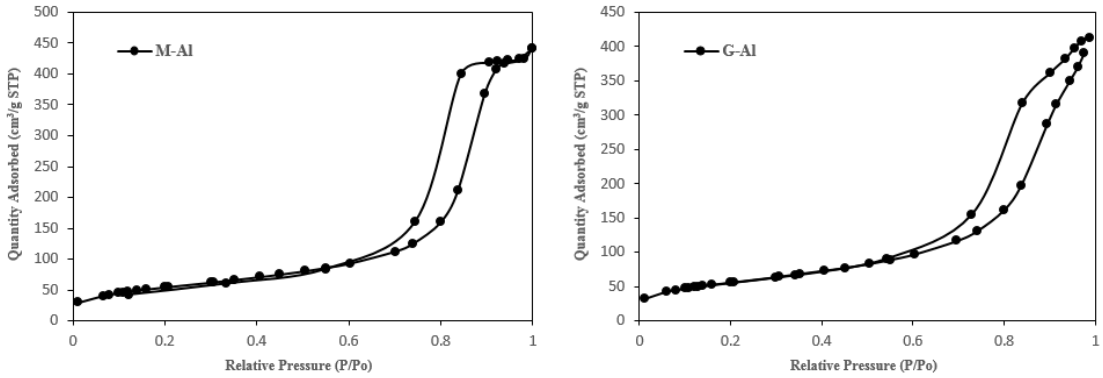

Figure 4.2 The N_2 adsorption–desorption isotherms of G-Al phase and M-Al phase catalysts

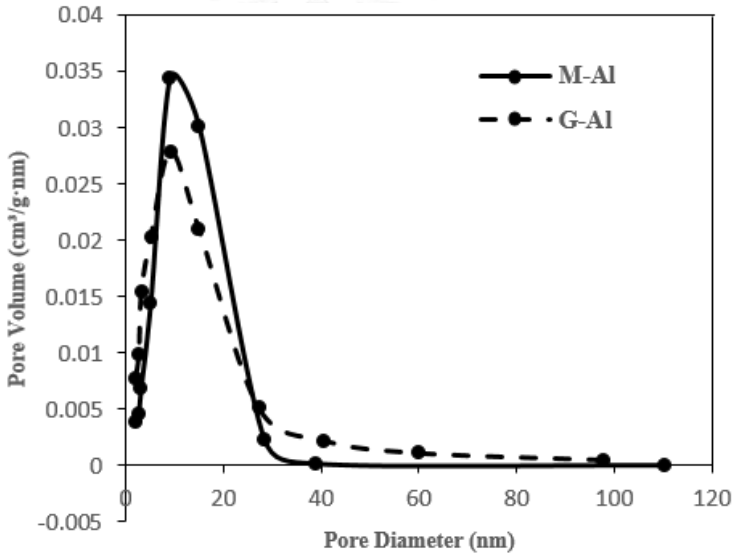

Figure 4.3 Pore size distribution of G-Al phase and M-Al phase catalysts

4.1.1.3 Temperature programmed adsorption (NH_3-TPD)

NH_3-TPD is one of the most powerful techniques for characterizing surface acidity of heterogeneous catalysts. The higher desorption temperature identifies to strong acid sites, corresponding to amount of NH_3 desorbed from under NH_3–TPD peak as shown in **Table 4.2**. In **Figure 4.4**, pure and mixed-phase alumina exhibited the amounts of weak acid sites and medium to strong acid sites at 100-220°C and 220-800°C, consecutively. The G-Al phase shows the amounts of weak acid sites nearby M-Al phase. On the other hand, the amounts of medium to strong acid sites become to lower, which affects to their quantity of total acidity. According to the phase transition, the morphology of G-Al phase is wrinkled sheets,

but the morphology of M-Al phase is wrinkled sheets mixed with spherical particles [55]. Therefore, the morphology may have effect on the total surface acidity of catalysts from 2.53 to 4.02 mmol NH_3/g cat. They are typically known as Lewis acid sites [22]. Moreover, the acid site was important to catalytic activity for ethanol dehydration into ethylene.

Table 4.2 Amount of NH_3 desorbed measured by area under the peak in different temperature range in the NH_3-TPD profile of G-Al phase and M-Al phase catalysts

Sample	NH_3 desorption (mmol NH_3/g cat.)		Total acidity (mmol NH_3 /g cat.)
	weak (100-220°C)	medium to strong (220-800°C)	
M-Al	2.76	4.02	6.78
G-Al	2.73	2.53	5.26

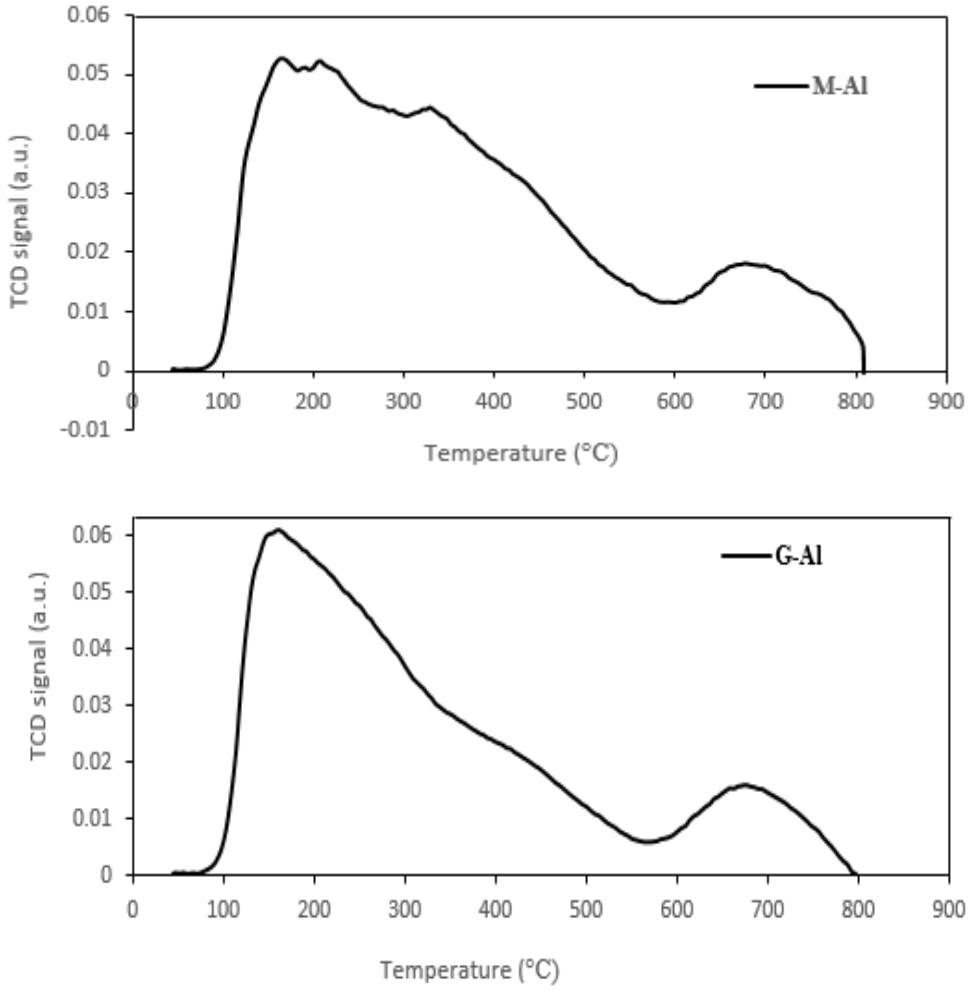

Figure 4.4 NH_3-TPD of G-Al phase and M-Al phase catalysts

4.1.2 Catalytic Activity

4.1.2.1 The stability of catalysts in ethanol dehydration reaction

The calcination temperature related to performance of mixed phase alumina catalysts. At calcination temperature of 600°C, it shows the best performance for ethanol dehydration reaction by temperature program in the range of 200°C to 400°C, corresponding with acidity properties that is the main factor of ethylene selectivity and ethanol conversion [55]. As the report, the ethylene formation prefers medium to stronger acid sites, whereas DEE prefers weak acid sites on solid catalyst. Therefore, the mixed phase alumina catalysts calcined at 600°C was chosen for the same tested reaction in time-on-stream condition. First, 0.05 g. of catalyst was put into the fixed-bed reactor at ambient pressure condition, and then vaporized ethanol was fed into the reactor by carrier gas. The ethanol injection flow rate is 1.45 ml/hr. Therefore, the weight hourly space velocity (WHSV) is defined as the ratio of the hourly feed molar flow rate of ethanol to the catalyst molar and kept at 22.88 hr^{-1}. The ethanol dehydration reaction was executed TOS at temperature of 300°C, 350°C and 400°C, respectively.

Normally, the catalytic activity depends on functional reaction temperature and time. According to the ethanol dehydration reaction theory, it has 2 reactions. The first reaction product is ethylene, which requires in main product and the second product is diethyl ether. Both of reactions have difference of thermodynamic potential follow equation in chapter 2. The enthalpy change (ΔH) is positive in endothermic reaction and negative in heat-releasing exothermic process. Moreover, the side reaction of ethanol reactant is dehydrogenation reaction, which also produces acetaldehyde product. Therefore, the ethylene product is studied majority of high temperature condition. The resulted reaction is displayed in **Figures 4.5** to **4.8**.

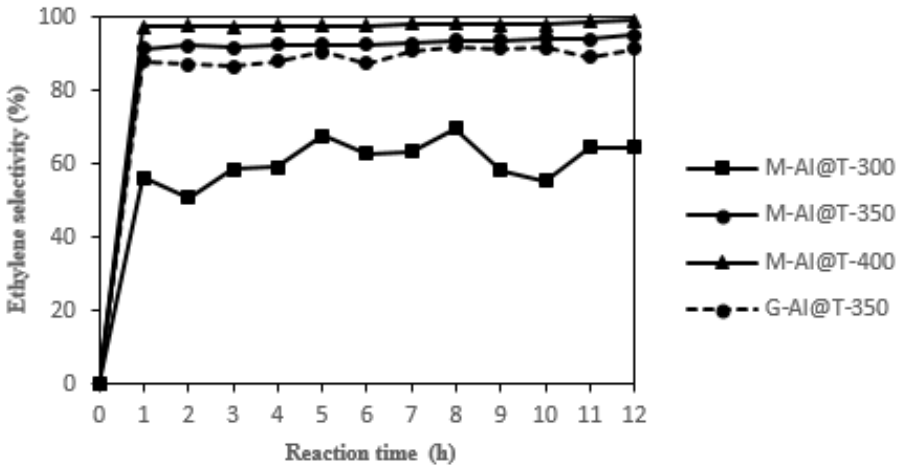

Figure 4.5 Ethylene selectivity of G-Al phase at 350°C and M-Al phase catalysts at 300°C, 350°C and 400°C for TOS 12 hrs.

Figures 4.5 to **4.7** show the relationship of selectivity versus time on stream over G-Al phase and M-Al phase catalysts. **Figure 4.5** exposes ethylene selectivity at several temperature. For M-Al catalyst, when temperature increased from 300°C to 400°C, it tends to increase the selectivity of ethylene. As a result, the average of ethylene selectivity at 1-12 hrs. was 61.0%, 93.1% and 98.0% at temperature 300°C, 350°C and 400°C, consecutively. The selectivity of ethylene was almost constant over 90% in during test time 12 hrs. at 350°C and 400°C. On the contrary, at temperature 300°C, it is observed slightly inconsistent selectivity of product, corresponding with endothermic reaction for ethanol dehydration reaction. For G-Al phase catalyst, it was only studied ethylene selectivity at temperature 350°C in order to compare status of transition phase. G-Al@T-350 displayed 89.5% selectivity at the same average of mixed phase. Therefore, when compared between M-Al phase and G-Al phase catalysts, the former appeared to have better activity. This result can be explained with acidity that has an effect on catalytic performance because the medium to strong acidity of M-Al phase greater than G-Al phase. However, the highest ethylene selectivity is presented on M-Al phase catalyst at temperature of 400°C.

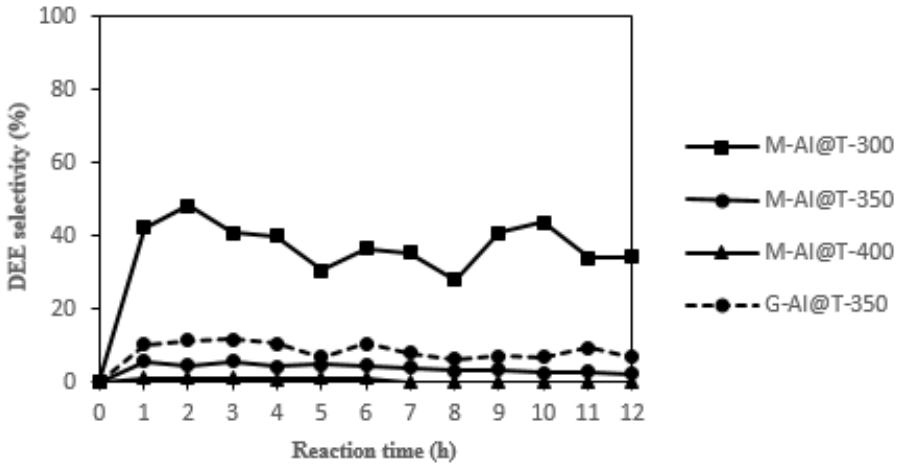

Figure 4.6 DEE selectivity of G-Al phase at 350°C and M-Al phase catalysts at 300°C, 350°C and 400°C for TOS 12 hrs.

Figure 4.6 shows selectivity of DEE at temperature 300°C, 350°C and 400°C. The lower temperature impacted on producing outgrowth diethyl ether. As the temperature increased, the selectivity to ethylene increased with a concomitant decrease in the selectivity to diethyl ether. The average of DEE selectivity at 1-12 hrs. was 37.9%, 4.0% and 0.6% at temperature 300°C, 350°C and 400°C for M-Al phase and 8.8% at temperature 350°C for G-Al phase, respectively. This is based on the fact that reaction to produce DEE is exothermic. Therefore, M-Al@T-300 exhibited highest DEE selectivity, but the output of both ethylene and DEE are not still smooth and stable at all reaction time. Moreover, in case of phase transition, the G-Al phase gave DEE selectivity higher than that of M-Al phase because of less amount of total acidity.

For the side reaction of ethanol reactant, besides dehydration reaction, dehydrogenation reaction can occur. Product obtained from this reaction is acetaldehyde having the selectivity as shown in **Figure 4.7**. The average selectivity displayed 1.2%, 2.9% and 1.4% at temperature 300°C, 350°C and 400°C for M-Al phase and 1.6% at temperature 350°C for G-Al phase, sequentially. Both M-Al phase and G-Al phase rendered the selectivity of acetaldehyde constantly under 3% at all temperature. This means that alumina catalyst is preferred for the dehydration reaction.

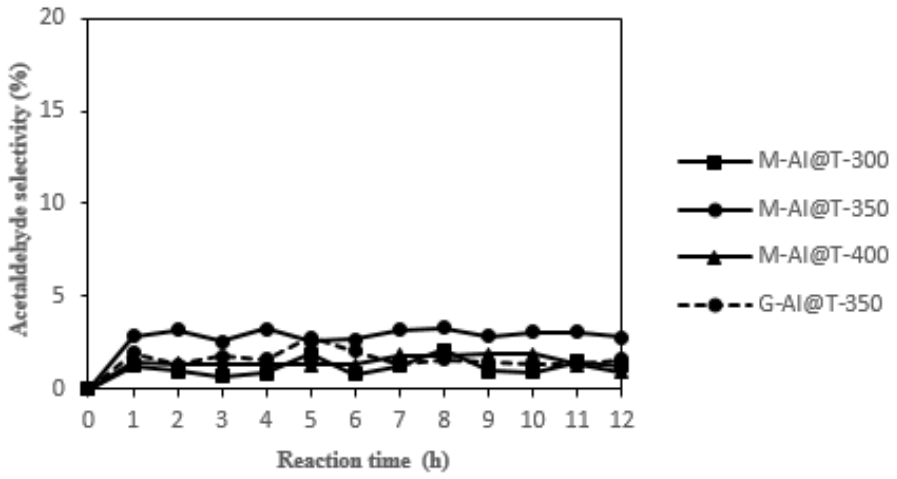

Figure 4.7 Acetaldehyde selectivity of G-Al phase at 350°C and M-Al phase catalysts at 300°C, 350°C and 400°C for TOS 12 hrs.

In **Figure 4.8**, it indicates relative reaction time versus ethanol conversion. The GC analysis was carried out at time on stream of 8 minutes. The catalysts were in order of ethanol conversion, M-Al@T-300 < G-Al@T-350 < M-Al@T-350 < M-Al@T-400, which were ca. 69.5%, 70.8%, 85.7% and 85.9% at average time. In the first period, the ethanol conversion shows a transient period before reaching a stable performance. Nevertheless, ethanol conversion increased around within the first 2 hrs. of reaction time. As a result, the catalyst performance is considered at stable profile after the transient period. Therefore, the G-Al phase and M-Al phase catalysts need to pre-treat by the flowing gaseous reactant for activation before the steady catalytic performance is reached. It affects a main product yield as the M-Al phase at temperature 400°C gave maximal yield. Although, M-Al@T-400 exhibits the best catalytic performance, it may rapidly deactivate by the coke formation. This cause will be discussed in the next section.

In preliminary experiment results, the modification of M-Al phase catalysts can improve activity having higher selectivity and conversion than G-Al phase catalyst. Obviously, G-Al phase displays ethanol conversion around 70%. On the other hand, the M-Al phase displays ethanol 85-90% of conversion, which is shifted to more ethylene product.

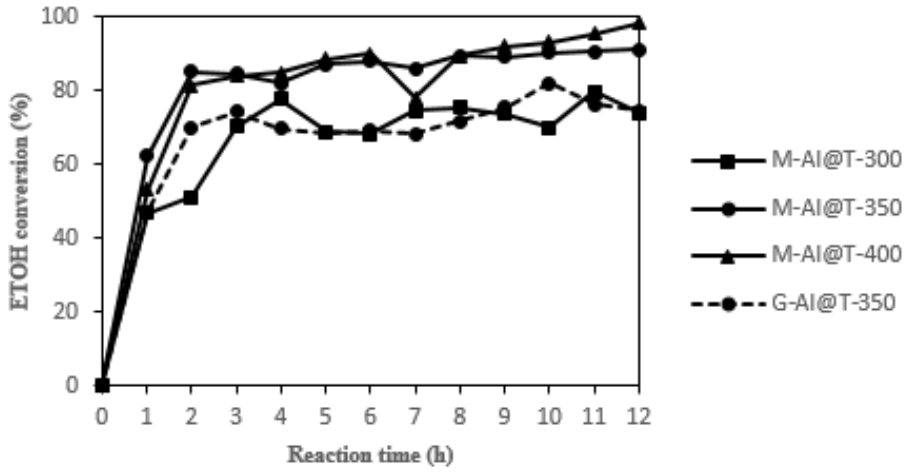

Figure 4.8 Ethanol conversion of G-Al phase at 350°C and M-Al phase catalysts at 300°C, 350°C and 400°C for TOS 12 hrs.

4.1.2.2 Deactivation of catalysts

The spent catalysts, which contained deposition at different levels after being used in ethanol dehydration reaction. As well known, the combustion of carbon species formed on spent catalysts can be measured by TG/DTG technique.

Table 4.3 Summarized amount of coke deposition on spent M-Al phase catalysts

Sample	Light coke weight loss (wt.%)	Heavy coke weight loss (wt.%)	Total weight loss (wt.%)
Temp = 300 °C TOS = 6 hrs.	3.14	0.79	6.98
Temp = 350 °C TOS = 6 hrs.	3.72	0.88	8.2
Temp = 400 °C TOS = 6 hrs.	3.89	0.84	7.21
Temp = 300 °C TOS = 12 hrs.	3.18	0.79	7.01
Temp = 350 °C TOS = 12 hrs.	4.3	0.96	8.64
Temp = 400 °C TOS = 12 hrs.	6.43	0.94	9.63

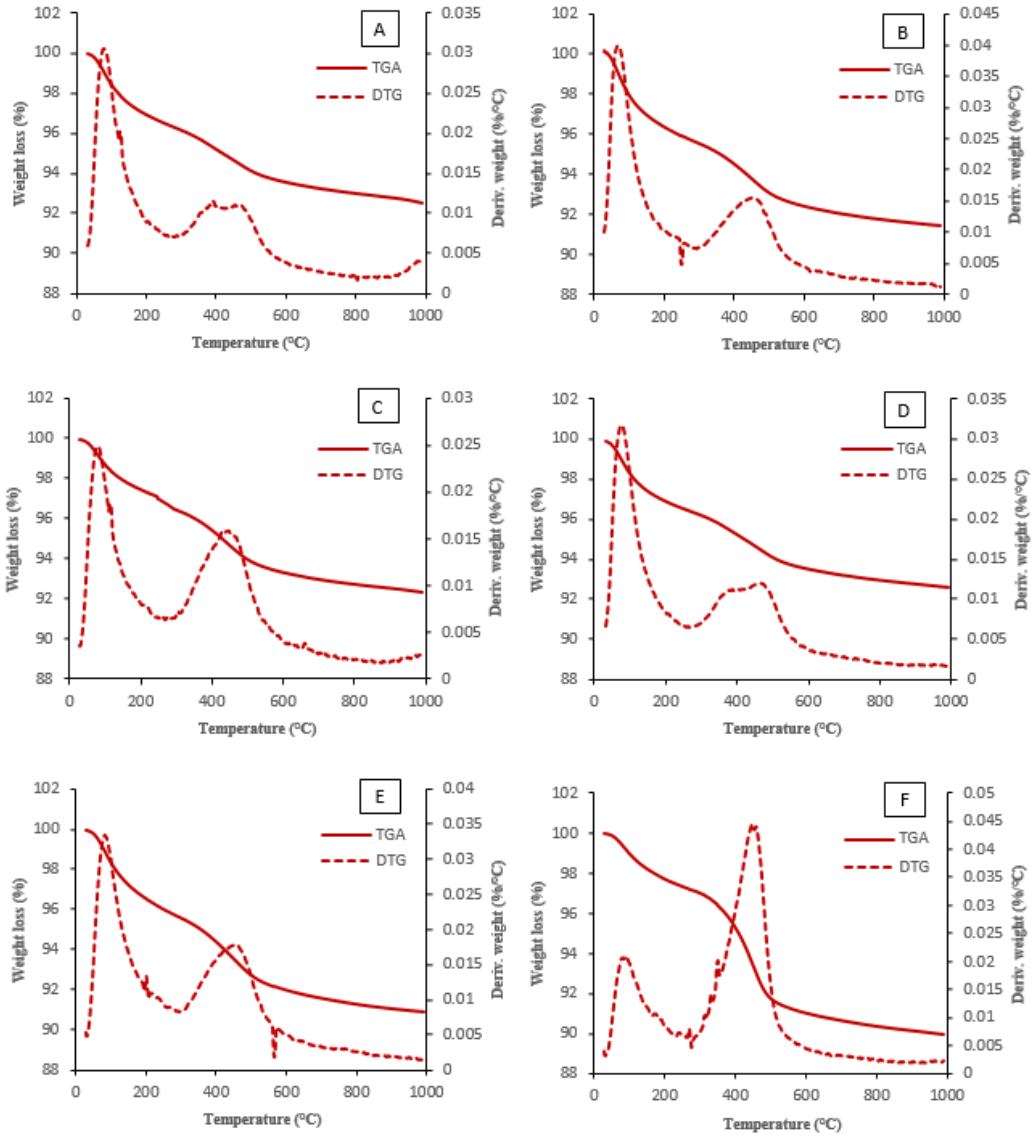

Figure 4.9 TG profile of spent M-Al phase catalysts in different reaction temperature: (A) T-300,6hrs., (B) T-350,6hrs., (C) T-400,6hrs., (D) T-300,12hrs., (E) T-350,12hrs. and (F) T-400,12hrs.

The TG analysis is performed in an oxidative atmosphere (air) with linear temperature ramp up. The maximum temperature is chosen, so that the sample weight is stable at the end of the experiment. Carbon is burnt off leaving aluminum oxides. The removal of coke deposits on M-Al phase catalyst can be calculated into weight loss (%) as a function of temperature. It was observed during the temperature less than 200°C, where this weight loss is attributed to the physically adsorbed water in the porous materials. Moreover, the weight loss of the light coke and the heavy coke are attributed to desorption in temperature between 200–550°C and 550–800°C, respectively. They seem that the light coke occurs from dehydration

and oligomerization in evident of heavy coke [56]. In **Figure 4.9**, the TG profiles expose two weight loss evident. The first evident represents water loss and the second evident reveals coke content by two features in the derivative curve. The amount of coke deposition on spent catalysts tends to increase after rising temperature and also increased reaction time. We can summarize the coke content in **Table 4.3**, where M-Al@T-400, 12 hrs. exhibits the highest coke content among other conditions. Furthermore, the weight loss of light coke is more than heavy coke in every samples. They mostly happen by the dehydration (the decomposition of ethylene and ethanol).

4.1.2.3 SEM-EDX of spent catalysts

The morphology of fresh and spent M-Al phase catalysts observed by SEM technique is shown in **Figure 4.10**. As a result, the surface of spent catalyst after TG analysis did not affect the morphologies of catalysts compared with a fresh catalyst. In fact, the characteristic morphology of coke reveals whisker carbon shape cover on a sample after run reaction [57]. However, after TG analysis, coke was almost removed from surface catalysts, thus they have similar morphology with the fresh catalyst.

The residual coke content, which was possibly permanent coke on solid catalyst can be detected using EDX technique and elemental composition of mixed phase alumina and the result is listed in **Table 4.4**. The residual coke continually increased as a function of temperature and time.

Table 4.4 EDX composition of spent M-Al phase catalysts after TG analysis

Sample	%Weight			%Atom		
	Al	O	C	Al	O	C
Fresh γ-χ Al_2O_3	53.29	46.71	-	40.35	59.65	-
Temp = 300 °C TOS = 6 hrs.	67.84	29.56	2.60	54.91	40.36	4.73
Temp = 350 °C TOS = 6 hrs.	59.85	37.08	3.07	47.47	47.28	5.25
Temp = 400 °C TOS = 6 hrs.	59.28	37.32	3.40	45.65	48.47	5.88
Temp = 300 °C TOS = 12 hrs.	64.84	31.95	3.21	51.49	42.78	5.72
Temp = 350 °C TOS = 12 hrs.	65.34	30.93	3.73	51.91	41.44	6.65
Temp = 400 °C TOS = 12 hrs.	66.48	28.73	4.79	52.89	38.54	8.57

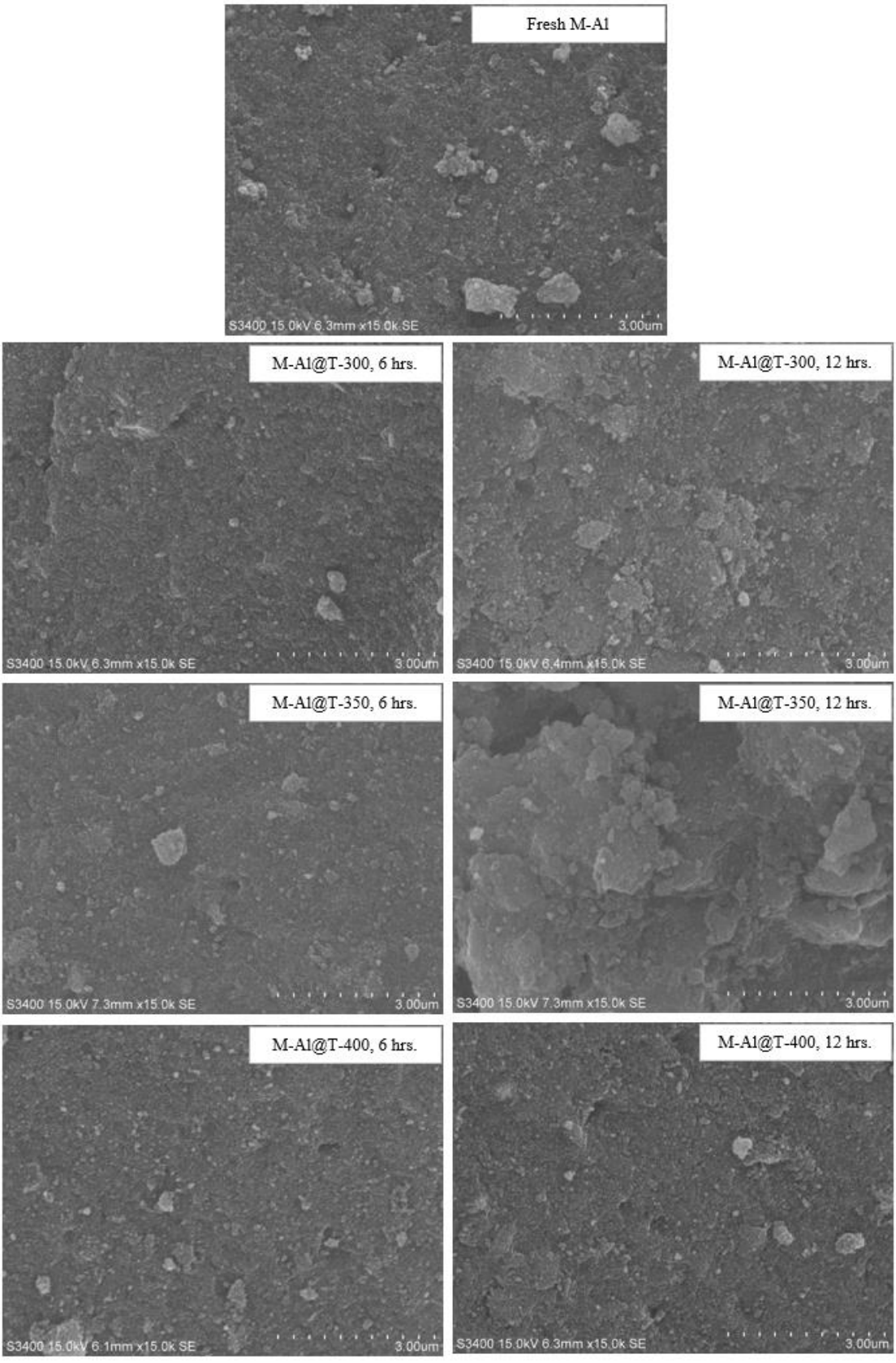

Figure 4.10 SEM micrograph of fresh and spent M-Al phase catalysts after TGA.

4.2 Characteristic and stability of 5wt% Mo-M-Al phase catalysts

4.2.1 Catalyst Characterization

4.2.1.1 X-ray diffraction (XRD)

The XRD patterns of Mo-M-Al phase catalyst was investigated to detect MoO_3 loading on M-Al phase catalyst synthesized via impregnation method using ammonium heptamolybdate tetrahydrate $(NH_4)_6Mo_7O_{24}\cdot 4H_2O$ for precursor. It was calcined in air at 500°C for 2 hrs. The crystalline structure of MoO_3 displayed an XRD profile with different diffraction peaks at 2θ = 12.868°, 23.408°, 25.788°, 27.408° and 39.068° [58]. The 5wt%Mo-containing catalyst (Mo-M-Al) is shown in **Figure 4.11**. Even though, it slightly detected Mo species, it obviously presented the main diffraction peak at 2θ = 27°. It is concluded that MoO_3 had well dispersed on alumina surface indicating of low intensity.

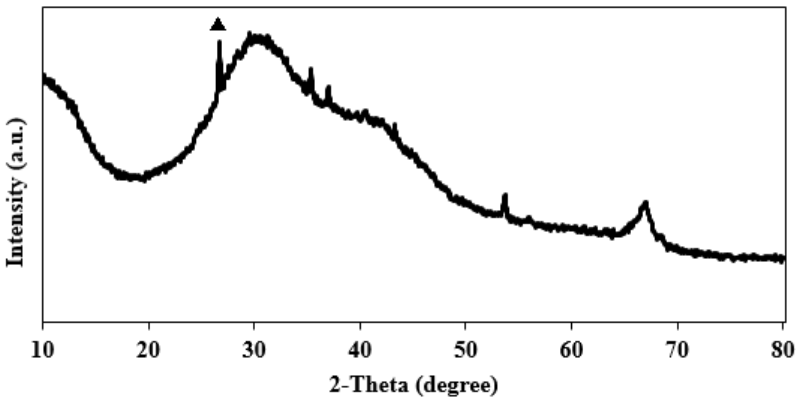

Figure 4.11 XRD patterns of Mo-M-Al phase catalyst; (▲) MoO_3 phase at 27°

4.2.1.2 Nitrogen physisorption

Table 4.5 summarizes the BET surface area, pore volume and pore size diameter for Mo-M-Al phase catalyst. As the result, the Mo-M-Al phase catalyst behaves smaller surface area than the M-Al phase catalyst (**Table 4.1**), which is due to a deposition of molybdenum species on the alumina surface. Furthermore, the Mo-M-Al phase catalyst exhibits a decrease of pore volume and pore size diameter as well. Many researches reported that the S_{BET}, P_V and P_d decreased with an increasing MoO_3 loading on supported [23, 55]. However, Mo-containing catalyst

was characterized as monolayer dispersion at low intensity. In **Figures 4.12-4.13**, they show the N_2 adsorption–desorption isotherms of modified Mo-M-Al phase. The feature corresponds to IV-type isotherms, indicating the mesoporous structure having pore size distribution in the range of 2-25 nm.

Table 4.5 BET surface area analysis and BJH pore size and volume analysis of Mo-M-Al phase catalyst.

Sample	BET surface area	Pore volume	Pore size diameter
	S_{BET} (m^2/g)	P_V (cm^3/g)	P_d (nm)
Mo-M-Al	190	0.47	6.30

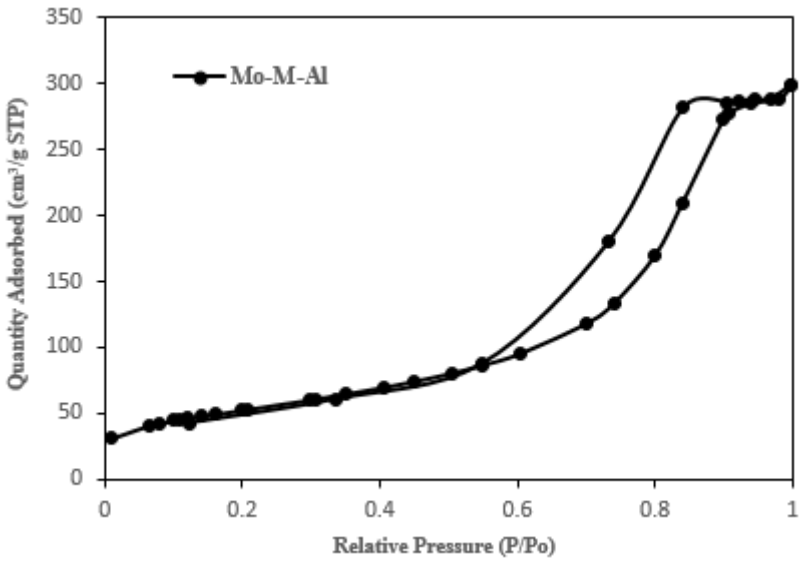

Figure 4.12 The N_2 adsorption–desorption isotherms of Mo-M-Al phase catalyst

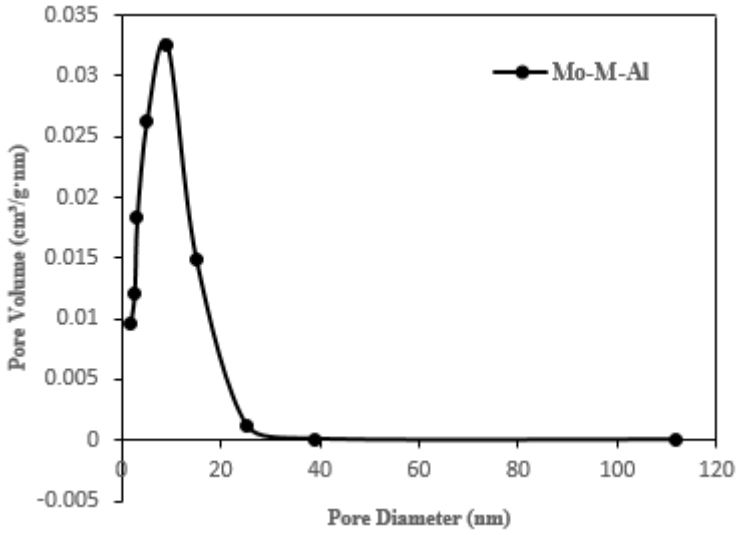

Figure 4.13 Pore size distribution of Mo-M-Al phase catalyst

4.2.1.3 Temperature programmed adsorption (NH_3-TPD)

According to the total acidity of M-Al phase in section 4.1, it showed 6.78 mmol NH_3/g cat. After the MoO_3 loading on mixed phase alumina catalysts, it tends to increase both weak to medium and strong acid sites as shown in **Table 4.6**, calculating from area under the peak of NH_3-TPD analysis in **Figure 4.14**. A strong acid is one that has a strong tendency to lose a proton. For Mo-M-Al phase, the total acidity was 11.43 mmol NH_3/g cat. The Mo loading apparently helped to promote the total acidity for M-Al phase. It corresponded with previous published abstract [55]. However, the increased acidity influences rapid deactivation over catalytic activity.

Table 4.6 Amount of NH_3 desorbed measured by area under the peak in different temperature range in the NH_3-TPD profile of Mo-M-Al phase and M-Al phase catalysts

Sample	**NH_3 desorption (mmol NH_3/g cat.)**		**Total acidity (mmol NH_3 /g cat.)**
	weak (100-220°C)	**medium to strong (220-800°C)**	
Mo-M-Al	3.59	7.84	11.43
M-Al	2.76	4.02	6.78

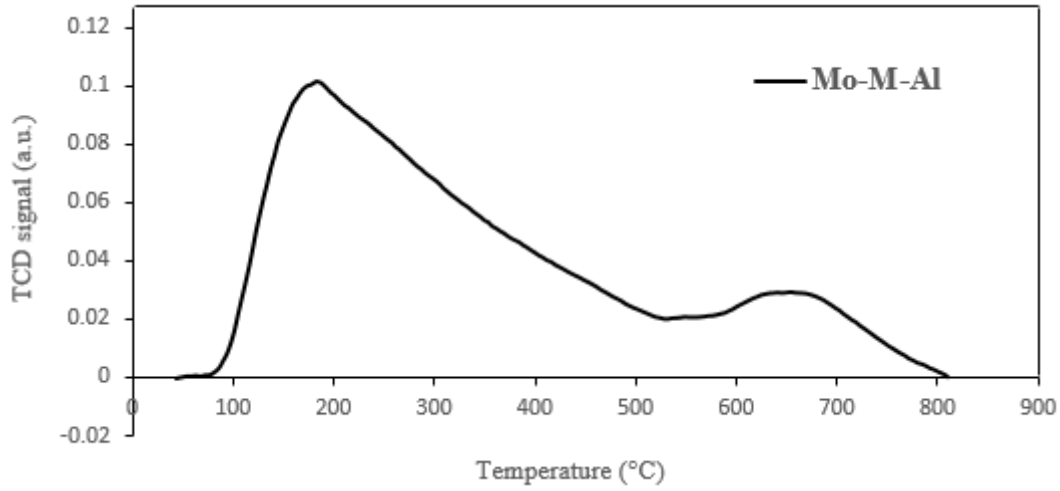

Figure 4.14 NH_3-TPD of Mo-M-Al phase catalysts

4.2.2 Catalytic Activity

4.2.2.1 The stability of catalysts in ethanol dehydration reaction

In this section, we investigated an improvement of total acidity on catalyst. For a previous report, the various modified MoO_3 loadings on mixed phase alumina catalysts from 5wt%, 10wt%, 15wt% and 20wt% were tested in ethanol dehydration reaction in condition of temperature program (200°C-400°C) [55]. It was found that 5wt%MoO_3/γ-χ-Al_2O_3 discovered the highest ethylene selectivity and ethanol conversion. On the contrary, when the percentage of MoO_3 loading increases on catalyst, the ethylene selectivity and ethanol conversion apparently decrease. Therefore, we are interested the modification of 5wt%MoO_3 to improve stability of Mo loading on catalyst.

The effect of reaction temperature at 300°C, 350°C and 400°C on the ethanol dehydration over Mo-M-Al catalysts was studied to determine the stability of modified catalyst. **Figures 4.15-4.17** show selectivity of G-Al phase and Mo-M-Al phase catalysts as a function of reaction time. With increasing temperature, the selectivity of ethylene increases with corresponding to theory and previous report [7]. The high reaction temperature encourages to the ethylene formation via intramolecular dehydration, whereas the low temperature attributes to intermolecular dehydration to DEE product.

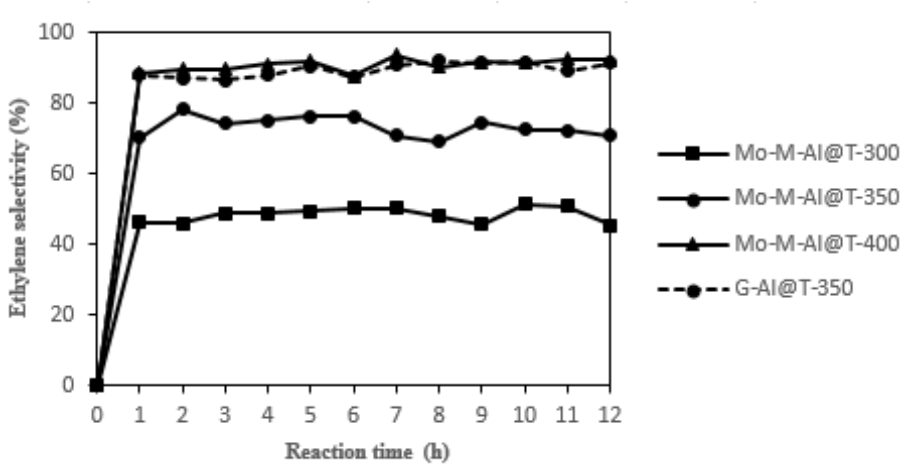

Figure 4.15 Ethylene selectivity of G-Al phase at 350°C and Mo-M-Al phase catalysts at 300°C, 350°C and 400°C for TOS 12 hrs.

The ethylene selectivity of modified MoO_3 catalyst at temperature 300°C, 350°C and 400°C were ca. 48.5%, 73.3% and 90.9% at during time on stream of 12 hrs. as shown in **Figure 4.15**. Aforementioned, the selectivity of G-Al phase catalyst is higher than Mo-M-Al phase catalyst at temperature 350°C. Therefore, when MoO_3 loading on catalyst, it results in decreased ethylene selectivity. This is due to Mo species promote the percentage of dehydrogenation reaction more than dehydration reaction [59]. The dehydrogenation reaction of ethanol yields hydrogen and acetaldehyde product. Even though the highest ethylene selectivity is presented at temperature of 400°C for Mo-M-Al phase catalyst, the mixed phase catalyst without MoO_3 content at the same temperature still has higher than Mo-M-Al.

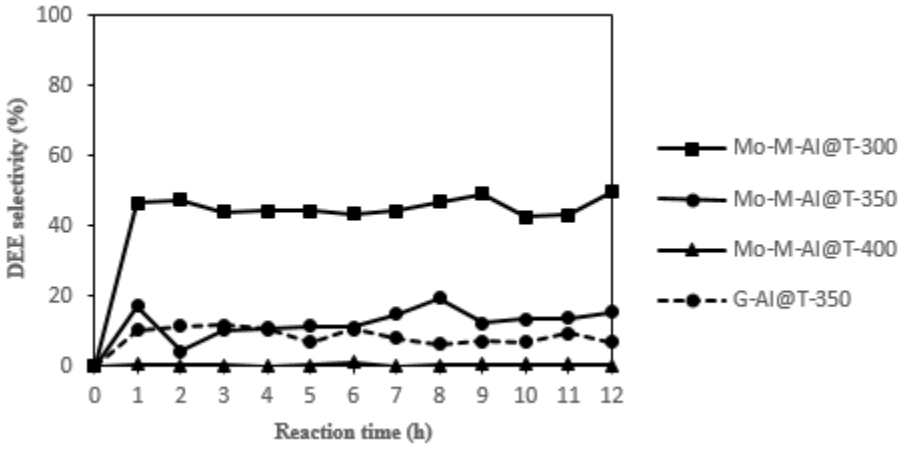

Figure 4.16 DEE selectivity of G-Al phase at 350°C and Mo-M-Al phase catalysts at 300°C, 350°C and 400°C for TOS 12 hrs.

Figure 4.16 displays DEE selectivity at temperature 300°C, 350°C and 400°C for TOS 12 hrs., which were 45.5%, 12.9% and 0.4%, respectively. The effective MoO_3 modification contributes to rise selectivity of DEE more than catalysts without modification. This result occurs from total acidity of Mo species with increasing in the amount of weak acid sites. As modified with MoO_3 at temperature of 300°C and 400°C, the selectivity of DEE were observed having smooth and steady curve, but Mo-M-Al@T-350 was quite unsteady during the stability test of TOS 12 hrs. It is possible to inspect the validity of shift to dehydrogenation reaction, which Mo sites promote higher acetaldehyde than that temperature at 300°C and 400°C as shown in **Figure 4.17**. This result may generate the unstable at result of DEE selectivity. The average of acetaldehyde selectivity was in order of Mo-M-Al@T-350 = 13.7% > Mo-M-Al@T-400 = 8.7% > Mo-M-Al@T-300 = 6.0% > G-Al@T-350 or M-Al phase catalysts as mentioned above. From this observation, the validity of the proposed mechanism for dehydration was cited as the highest acetaldehyde at temperature of 350°C for Mo-M-Al phase because when temperature become lower, Mo-M-Al@T-300 shifted to obtain more DEE selectivity owing to more effect of alumina catalyst. On the other hand, temperature increasing, Mo-M-Al@T-400 shifted to obtain more ethylene selectivity. However, ethylene selectivity of Mo-M-Al@T-400 still higher than Mo-M-Al@T-300, because the reaction of ethanol to acetaldehyde is endothermic reaction. For Mo-M-Al@T-350, it was not obvious for both DEE and ethylene selectivity. Therefore, it exhibited high selectivity of acetaldehyde more than others.

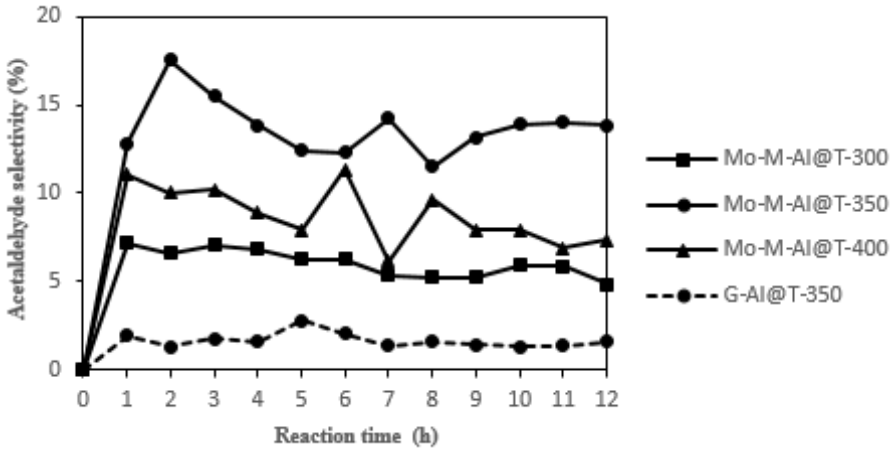

Figure 4.17 Acetaldehyde selectivity of G-Al phase at 350°C and Mo-M-Al phase catalysts at 300°C, 350°C and 400°C for TOS 12 hrs.

From **Figure 4.18**, it reveals the ethanol conversions in the order of; Mo-M-Al@T-400 > Mo-M-Al@T-350 > Mo-M-Al@T-300, which are 93.2%, 71.7% and 46.2% for average TOS 12 hrs. At Mo-M-Al@T-400 condition, after an initial period of approximately 2 hrs., the conversion remains essentially constant with time on stream. On the other hand, both Mo-M-Al@T-300 and Mo-M-Al@T-350 seemed unsteady in term of stability. Mo-M-Al@T-350 may occurs from Mo species that drop active sites of γ-χ-Al_2O_3, because selectivity of Mo sites favor dehydrogenation more than dehydration reaction as mentioned above and also more coke formation. Nevertheless, when reaction temperature increases, the conversion of ethanol also increases. The catalytic performance of Mo-M-Al did not show noticeable decay after reaction for 12 hrs.

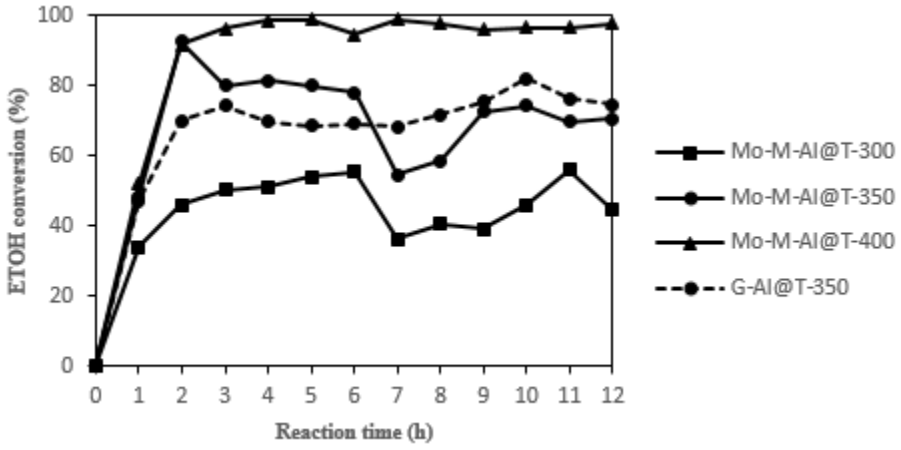

Figure 4.18 Ethanol conversion of G-Al phase at 350°C and Mo-M-Al phase catalysts at 300°C, 350°C and 400°C for TOS 12 hrs.

4.2.2.2 Deactivation of catalysts

TG/DTG technique can be used to measure the coke formation covering on the surface catalyst by measuring the weight loss as seen in **Figure 4.19,** and then calculate the light coke and heavy coke weight loss at temperature between 200-550°C and 550-800°C, respectively. It is shown in **Table 4.7**.

Table 4.7 Summarized amount of coke deposition on spent Mo-M-Al catalysts

Sample	Light coke weight loss (wt.%)	Heavy coke weight loss (wt.%)	Total weight loss (wt.%)
Temp = 300 °C TOS = 6 hrs.	3.27	0.61	6.25
Temp = 350 °C TOS = 6 hrs.	4.12	0.68	6.88
Temp = 400 °C TOS = 6 hrs.	6.66	0.62	9.35
Temp = 300 °C TOS = 12 hrs.	3.38	0.71	6.46
Temp = 350 °C TOS = 12 hrs.	7.99	0.59	10.91
Temp = 400 °C TOS = 12 hrs.	7.27	0.65	10.61

Amount of coke on the spent Mo-M-Al catalysts was almost found in the range of light coke weight loss because the products generated from dehydration reaction is small chain hydrocarbon. Therefore, amount of weight loss could be measured based on the light coke more than heavy coke. As the results, light coke content increased following several conditions such as temperature, TOS, acidity and involved effect of MoO_3 loading that converts to acetaldehyde product. It possibly generated the highest light coke at temperature of 350°C.

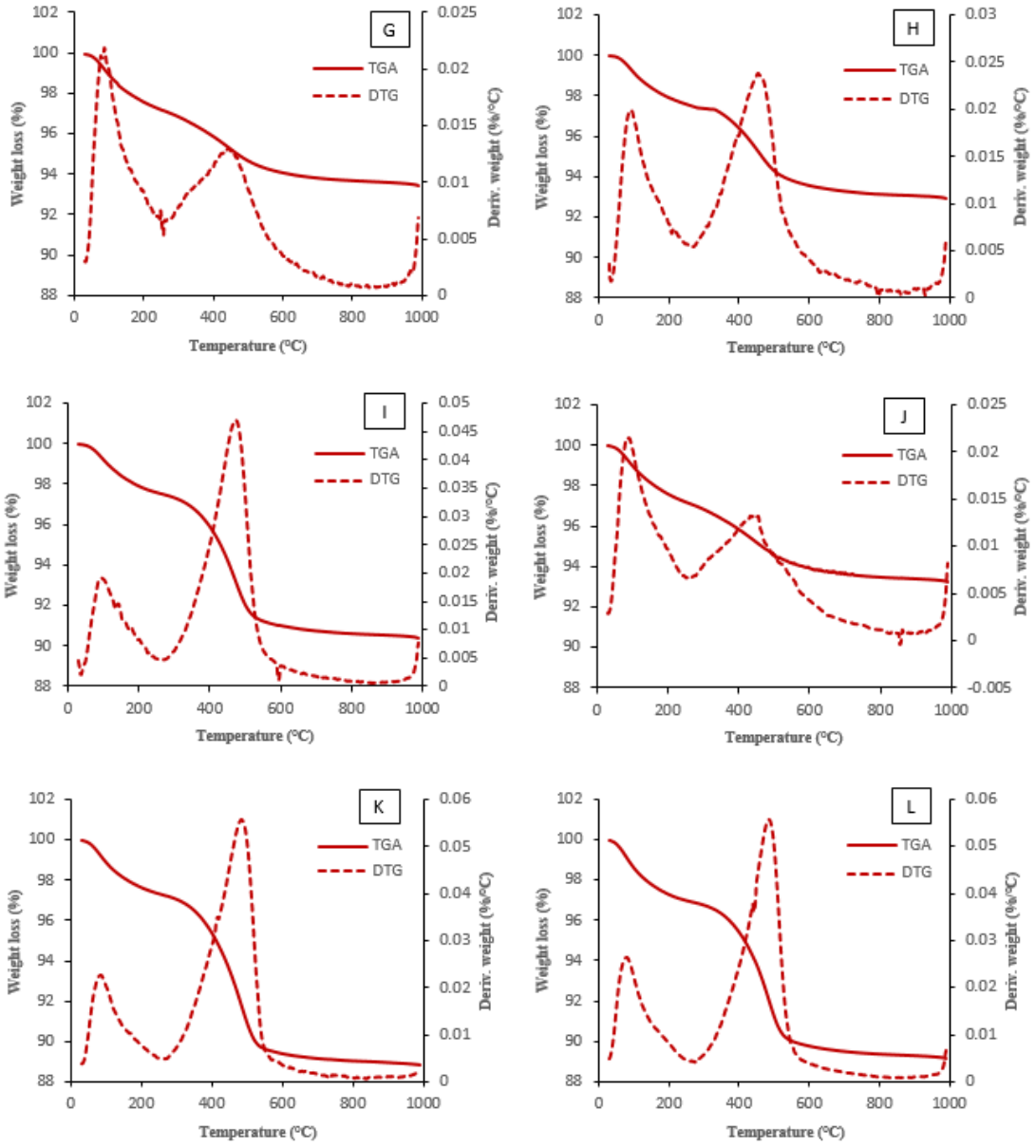

Figure 4.19 TG profiles of spent Mo-M-Al catalysts in different reaction temperatures: (G) T-300,6hrs., (H) T-350,6hrs., (I) T-400,6hrs., (J) T-300,12hrs., (K) T-350,12hrs. and (L) T-400,12hrs.

4.2.2.3 SEM-EDX of spent catalysts

The morphology of fresh and spent Mo-M-Al catalysts is presented in **Figure4.20**. When Mo-M-Al was compared with M-Al, it was found that the Mo-M-Al surface showed aggregation of MoO_3 on the catalyst. Mo-M-Al was possibly well dispersion with 5wt% if metal oxide was not observed in XRD patterns (**Figure 4.11**). However, amount of coke was observed by SEM technique after TG

analysis. They had the same fresh morphology like a M-Al catalysts. For the coke residue on Mo-M-Al can be investigated by EDX technique as shown in **Table 4.8**. At the first period (TOS = 6hrs.), the coke content tended to increase as a function of temperature and time, but after the first period (TOS = 12 hrs.), the residual coke of Mo-M-Al seemed to occur very fast and more than M-Al catalysts, thus the MoO_3 modification possibly influenced on coke formation corresponding with TG analysis.

Table 4.8 EDX composition of spent Mo-M-Al catalysts after TG analysis

Sample	%Weight				%Atom			
	Al	**O**	**Mo**	**C**	**Al**	**O**	**Mo**	**C**
Fresh Mo-M-Al	53.75	41.65	4.6	-	42.90	56.06	1.03	-
Temp = 300 °C TOS = 6 hrs.	52.86	37.08	7.46	2.60	43.37	50.18	1.72	4.73
Temp = 350 °C TOS = 6 hrs.	53.87	34.42	6.01	5.7	42.61	45.92	1.34	10.13
Temp = 400 °C TOS = 6 hrs.	54.24	32.77	5.95	7.03	42.72	43.52	1.32	12.44
Temp = 300 °C TOS = 12 hrs.	47.51	34.85	8.39	9.25	38.24	50.61	1.90	9.25
Temp = 350 °C TOS = 12 hrs.	54.83	27.87	7.24	10.06	43.36	37.17	1.61	17.87
Temp = 400 °C TOS = 12 hrs.	56.24	28.49	5.24	10.04	43.83	37.44	1.15	17.58

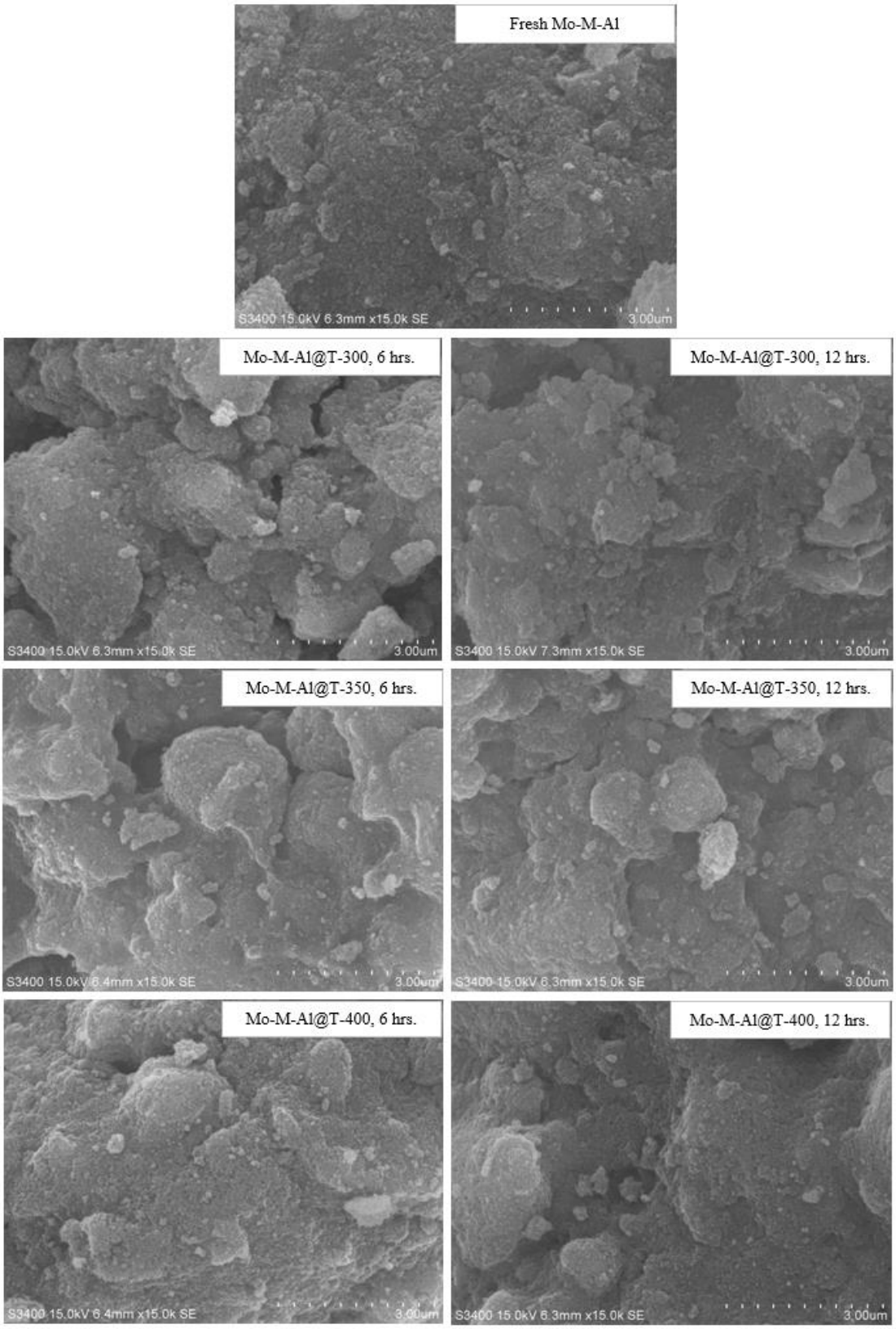

Figure 4.20 SEM micrograph of fresh and spent Mo-M-Al catalysts after TGA.

4.3 Catalytic performance of M-Al, G-Al and Mo-M-Al

The catalytic performance of all catalysts is presented in **Table 4.9**. The ethanol activity reached a steady state after the reaction was run about 2 hrs. Therefore, we analysed ethylene, DEE and acetaldehyde yield during average TOS of 3-12 hrs. These results can be explained that the best reaction temperature ascribed to the highest ethylene yield at 400°C was found higher than 80%. However, coke generated increased with increased temperature and reaction time. This deactivation can be related to a blockage by coke deposition of the access of the reactant to the alumina pores. Therefore, we compared and found optimum operating condition for M-Al phase.

Table 4.9 Summarized catalytic performance

Sample	Selectivity (%) [I]			Yield (mole %) [II]		
	Ethylene	**DEE**	**Acetaldehyde**	**Ethylene**	**DEE**	**Acetaldehyde**
M-Al @T-300	62.41	36.40	1.19	45.73	26.63	0.88
M-Al @T-350	93.30	3.79	2.91	81.97	3.31	2.56
M-Al @T-400	98.06	0.49	1.46	87.60	0.42	1.30
G-Al @T-350	89.87	8.47	1.66	65.59	6.17	1.20
Mo-M-Al @T-300	48.91	45.22	5.87	23.21	21.32	2.81
Mo-M-Al @T-350	73.19	13.34	13.47	52.85	9.41	9.71
Mo-M-Al @T-400	91.18	0.40	8.42	88.59	0.38	8.16

Note: I. Average at TOS 3-12 hrs.
II. Yield (%) = Ethanol conversion (%) × Selectivity (%)

4.3.1 Yield of M-Al, G-Al and Mo-M-Al catalysts

- For transition phase at temperature 350°C, ethylene yields of M-Al and G-Al catalysts were approximately estimate 82% and 66%, respectively. It can be concluded that the phase transition affects catalytic activity because selectivity

varies with total acidity of each catalyst, where the total acidity of M-Al was 6.78 mmol NH_3/g cat. and G-Al was 5.26 mmol NH_3/g cat.

- For M-Al catalyst at different temperatures, T-350 and T-400 exposed ethylene yield ~ 82% and 88%, consecutively. The temperature condition is well-known to have an effect on ethylene selectivity.
- For Mo-M-Al catalyst at different temperatures, T-350 and T-400 exposed ethylene yield ~ 53% and 89%, consecutively. This result is similar as mentioned above.
- Mo-M-Al catalyst promoted acetaldehyde selectivity more than M-Al catalyst which resulted in a lost of selectivity yield of main product excepting for Mo-M-Al@T-400. It showed the highest selectivity yield because of temperature and MoO_3 loading.

4.3.2 Stability of M-Al and Mo-M-Al catalysts

- M-Al@T-350 and M-Al@T-400 catalysts discovered light coke weight loss around 4.30wt% and 6.43wt% at TOS of 12 hrs. Amount of coke formation affects M-Al@T-400 catalyst which was less stable than M-Al@T-350.
- Mo-M-Al@T-350 and Mo-M-Al@T-400 catalysts detected light coke weight loss around 7.99wt% and 7.27wt% at TOS of 12 hrs. Mo-M-Al@T-350 possibly produced coke content more than Mo-M-Al@T-400 due to the highest acetaldehyde. These coke formation based on temperature, TOS, acid site and etc. Therefore, when coke increases, product yield and stability decreases. Finally, the best effective catalyst was proposed to be M-Al@T-350.

4.3.3 Economics impact of the M-Al catalyst

- The M-Al catalyst exhibits the greatest feature in case of yield, selectivity and deactivation among other catalysts. Both M-Al@T-350 and M-Al@T-400 presented ethylene yield over 80% and low coke formation at TOS = 12 hrs.

Therefore, we create assumption for catalytic deactivation for both candidates in order to predict and find optimal condition as follows:

The minimum stability of TOS was assumed to be 13 hrs. for M-Al@T-350 and 12 hrs. for M-Al@T-400 before degradation. The M-Al@T-350 was proposed for the condition of TOS more than other one due to its few coke formation. Thus, the ethylene product of the samples can be calculated form following formulas:

Ethylene product = Ethanol feed × Ethylene yield (5)

where: Feed = 1.45 cc/hr. (lab scale)

Moreover, we can approximately predict the electrical energy at temperature 350°C and 400°C as follow calculation formula:

P (watt) = I (A) × V (volt) (6)

E (unit) = P (kW) × time (hours) (7)

where "I" denotes SANGI SGA 225 Output Relay = 25 A. (assume total load is 25 A. at peak temperature 400°C), "V" input voltage = 220 Volt.

Table 4.10 The effective of catalysts between M-Al@T-350 and M-Al@T-400

Sample	Ethylene yield (%)	Ethylene product (cc.)	Power (kW)	Electrical Energy (Unit)
M-Al@T-350[III]	81.97	15.45	4.813	62.56
M-Al@T-400[VI]	87.60	15.24	5.5	66.00

Note: III. Assumption TOS at 13 hrs.
VI. Assumption TOS at 12 hrs.

As mentioned above, the best catalytic performance of the mixed γ- and χ-crystalline phase alumina catalyst was observed at 350°C as shown in **Table 4.10**.

CHAPTER V
CONCLUSIONS AND RECOMMENDATION

This chapter V was summarized about characteristic and stability of M-Al, G-Al and Mo-M-Al phase catalysts for ethanol dehydration reaction, which described in section 5.1. Furthermore, the section 5.2 was mentioned recommendation for additional research to cover the result.

5.1 Conclusions

1. The phase transition affects catalytic activity, where the total acidity of mixed γ- and χ- phase is more than pure γ-phase Al_2O_3. While MoO_3 loading influenced to the highest of total acidity of others catalyst.
2. At temperature of 350°C, the ethylene yield of M-Al phase exposed it was higher than G-Al phase because of effect on acid site. On the other hand, Mo-M-Al exhibited less the ethylene yield than others catalyst at 350°C. Because the metal oxide of MoO_3 favors dehydrogenation reaction, which it was converted from ethanol to more acetaldehyde instead of promoted to ethylene.
3. The coke formation based on acidity of catalyst, increased temperature and reaction time. The coke obstructed the access of ethanol to the alumina pores, which it becomes to deactivate performance of catalyst.
4. The ethanol conversion of alumina catalyst reveals a transient period before reaching a stable performance within the first 2 hrs. of reaction time. Therefore, the alumina catalyst requires pre-treat by ethanol gaseous for activation.
5. Stability of M-Al phase catalyst at temperature of 350°C was observed that it was suitable for catalytic activity in ethanol dehydration reaction.

5.2 Recommendations

1. The amount of coke formation should also be measured by temperature-programmed oxidation method with IR detection (TPO-IR) specifically for the analysis of CO_2 released.
2. The solution of regenerate catalyst should be studied and investigated catalytic activity in ethanol dehydration reaction after regenerated coke.

3. The final reaction time before catalytic deactivation should be more researched in order to prove the accuracy of optimum operating temperature.
4. The amount of ethanol flow rate should be studied how it affects ethylene selectivity in dehydration reaction.

REFERENCES

1. Starokon, E.V., et al., *Epoxidation of ethylene by anion radicals of α-oxygen on the surface of FeZSM-5 zeolite.* Journal of Catalysis, 2014. **309**(0): p. 453-459.
2. Shi, Y.-f., et al., *Kinetics for benzene+ethylene reaction in near-critical regions.* Chemical Engineering Science, 2001. **56**(4): p. 1403-1410.
3. Sastri, V.R., *6 - Commodity Thermoplastics: Polyvinyl Chloride, Polyolefins, and Polystyrene*, in *Plastics in Medical Devices (Second Edition)*, V.R. Sastri, Editor. 2014, William Andrew Publishing: Oxford. p. 73-120.
4. True, W.R. 2013; Available from: www.ogj.com/articles/print/volume-111/issue-7/special-report-ethylene-report/global-ethylene-capacity-poised-for-major.html.
5. Sadrameli, S.M., *Thermal/catalytic cracking of hydrocarbons for the production of olefins: A state-of-the-art review I: Thermal cracking review.* Fuel, 2015. **140**(0): p. 102-115.
6. Zhang, M. and Y. Yu, *Dehydration of ethanol to ethylene.* Industrial & Engineering Chemistry Research, 2013. **52**(28): p. 9505-9514.
7. Zhang, X., et al., *Comparison of four catalysts in the catalytic dehydration of ethanol to ethylene.* Microporous and Mesoporous Materials, 2008. **116**(1–3): p. 210-215.
8. Bedia, J., et al., *Ethanol dehydration to ethylene on acid carbon catalysts.* Applied Catalysis B: Environmental, 2011. **103**(3–4): p. 302-310.
9. Jenness, G.R., et al., *Site-Dependent Lewis Acidity of γ-Al2O3 and Its Impact on Ethanol Dehydration and Etherification.* The Journal of Physical Chemistry C, 2014. **118**(24): p. 12899-12907.
10. Golay, S., R. Doepper, and A. Renken, *Reactor performance enhancement under periodic operation for the ethanol dehydration over γ-alumina, a reaction with a stop-effect.* Chemical Engineering Science, 1999. **54**(20): p. 4469-4474.
11. Chen, Y., et al., *Dehydration reaction of bio-ethanol to ethylene over modified SAPO catalysts.* Journal of Industrial and Engineering Chemistry, 2010. **16**(5): p. 717-722.
12. Golay, S., R. Doepper, and A. Renken, *In-situ characterisation of the surface intermediates for the ethanol dehydration reaction over γ-alumina under dynamic conditions.* Applied Catalysis A: General, 1998. **172**(1): p. 97-106.
13. Phung, T.K., et al., *A study of commercial transition aluminas and of their catalytic activity in the dehydration of ethanol.* Journal of Catalysis, 2014. **311**(0): p. 102-113.
14. *Dehydration of Alcohols*. Available from: http://www.mhhe.com/physsci/chemistry/carey5e/Ch05/ch5-2.html.
15. Kito-Borsa, T. and S. Cowley, *Kinetics, Characterization and mechanism for the selective dehydration of ethanol to diethyl ether over solid acid catalysts.* 2004.
16. *Alcohols, Diols and Thiols*. Available from: http://www.mhhe.com/physsci/chemistry/carey/student/olc/ch15synthesisethers.html.

17. Wu, L.-P., et al., *The fabrication of TiO2-supported zeolite with core/shell heterostructure for ethanol dehydration to ethylene.* Catalysis Communications, 2009. **11**(1): p. 67-70.
18. Chorkendorff, I. and J.W. Niemantsverdriet, *Concepts of modern catalysis and kinetics*. 2006: John Wiley & Sons.
19. Carter, C.B. and M.G. Norton, *Ceramic materials: science and engineering*. 2007: Springer Science & Business Media.
20. Shirai, T., et al., *Structural properties and surface characteristics on aluminum oxide powders.* Ceramics Research Lab, 2009. **9**: p. 23-31.
21. Li, Z., *Novel solid base catalysts for Michael additions*, 2005, Humboldt-Universität zu Berlin, Mathematisch-Naturwissenschaftliche Fakultät I.
22. Santacesaria, E., D. Gelosa, and S. Carrà, *Basic behavior of alumina in the presence of strong acids.* Industrial & Engineering Chemistry Product Research and Development, 1977. **16**(1): p. 45-47.
23. Solsona, B., et al., *Molybdenum–vanadium supported on mesoporous alumina catalysts for the oxidative dehydrogenation of ethane.* Catalysis Today, 2006. **117**(1–3): p. 228-233.
24. El-Sharkawy, E.A., A.S. Khder, and A.I. Ahmed, *Structural characterization and catalytic activity of molybdenum oxide supported zirconia catalysts.* Microporous and Mesoporous Materials, 2007. **102**(1–3): p. 128-137.
25. Bartholomew, C.H., *Mechanisms of catalyst deactivation.* Applied Catalysis A: General, 2001. **212**(1): p. 17-60.
26. Wang, F., et al., *Coking behavior of a submicron MFI catalyst during ethanol dehydration to ethylene in a pilot-scale fixed-bed reactor.* Applied Catalysis A: General, 2011. **393**(1–2): p. 161-170.
27. Hu, H., et al., *Study of coke behaviour of catalyst during methanol-to-olefins process based on a special TGA reactor.* Chemical Engineering Journal, 2010. **160**(2): p. 770-778.
28. Al-Zeghayer, Y.S. and B.Y. Jibril, *On the effects of calcination conditions on the surface and catalytic properties of γ-Al2O3-supported CoMo hydrodesulfurization catalysts.* Applied Catalysis A: General, 2005. **292**(0): p. 287-294.
29. Ozawa, M. and Y. Nishio, *Thermal stabilization of γ-alumina with modification of lanthanum through homogeneous precipitation.* Journal of Alloys and Compounds, 2004. **374**(1–2): p. 397-400.
30. Seo, Y.-S., et al., *The effect of Ni content on a highly active Ni–Al2O3 catalyst prepared by the homogeneous precipitation method.* International Journal of Hydrogen Energy, 2011. **36**(1): p. 94-102.
31. Sivakumar, S., et al., *Nanoporous titania–alumina mixed oxides—an alkoxide free sol–gel synthesis.* Materials Letters, 2004. **58**(21): p. 2664-2669.
32. Wang, W., et al., *Different surfactants-assisted hydrothermal synthesis of hierarchical γ-Al2O3 and its adsorption performances for parachlorophenol.* Chemical Engineering Journal, 2013. **233**(0): p. 168-175.
33. Wang, H., et al., *Highly dispersed NiW/γ-Al2O3 catalyst prepared by hydrothermal deposition method.* Catalysis Today, 2007. **125**(3–4): p. 149-154.

34. Jeon, M.-K. and M. Kang, *Synthesis and characterization of indium-tin-oxide particles prepared using sol–gel and solvothermal methods and their conductivities after fixation on polyethyleneterephthalate films.* Materials Letters, 2008. **62**(4–5): p. 676-682.
35. Walton, R.I., *Solvothermal synthesis of cerium oxides.* Progress in Crystal Growth and Characterization of Materials, 2011. **57**(4): p. 93-108.
36. Li, G., et al., *Synthesis of flower-like Boehmite (AlOOH) via a simple solvothermal process without surfactant.* Materials Research Bulletin, 2010. **45**(10): p. 1487-1491.
37. Phung, T.K., L. Proietti Hernández, and G. Busca, *Conversion of ethanol over transition metal oxide catalysts: Effect of tungsta addition on catalytic behaviour of titania and zirconia.* Applied Catalysis A: General, 2015. **489**(0): p. 180-187.
38. Ramesh, K., et al., *Structure and reactivity of phosphorous modified H-ZSM-5 catalysts for ethanol dehydration.* Catalysis Communications, 2009. **10**(5): p. 567-571.
39. Sheng, Q., et al., *Effect of steam treatment on catalytic performance of HZSM-5 catalyst for ethanol dehydration to ethylene.* Fuel Processing Technology, 2013. **110**(0): p. 73-78.
40. Bi, J., et al., *High effective dehydration of bio-ethanol into ethylene over nanoscale HZSM-5 zeolite catalysts.* Catalysis Today, 2010. **149**(1–2): p. 143-147.
41. Xin, H., et al., *Catalytic dehydration of ethanol over post-treated ZSM-5 zeolites.* Journal of Catalysis, 2014. **312**(0): p. 204-215.
42. Bokade, V.V. and G.D. Yadav, *Heteropolyacid supported on montmorillonite catalyst for dehydration of dilute bio-ethanol.* Applied Clay Science, 2011. **53**(2): p. 263-271.
43. Varisli, D., T. Dogu, and G. Dogu, *Ethylene and diethyl-ether production by dehydration reaction of ethanol over different heteropolyacid catalysts.* Chemical Engineering Science, 2007. **62**(18–20): p. 5349-5352.
44. Wang, Y., J. Liu, and W. Li, *Synthesis of 2-butoxy ethanol with narrow-range distribution catalyzed by supported heteropolyacids.* Journal of Molecular Catalysis A: Chemical, 2000. **159**(1): p. 71-75.
45. Alharbi, W., et al., *Dehydration of ethanol over heteropoly acid catalysts in the gas phase.* Journal of Catalysis, 2014. **319**(0): p. 174-181.
46. DeWilde, J.F., et al., *Kinetics and Mechanism of Ethanol Dehydration on γ-Al2O3: The Critical Role of Dimer Inhibition.* ACS Catalysis, 2013. **3**(4): p. 798-807.
47. El-Katatny, E.A., et al., *Recovery of ethene-selective FeOx/Al2O3 ethanol dehydration catalyst from industrial chemical wastes.* Applied Catalysis A: General, 2000. **199**(1): p. 83-92.
48. Chen, G., et al., *Catalytic dehydration of bioethanol to ethylene over TiO2/γ-Al2O3 catalysts in microchannel reactors.* Catalysis Today, 2007. **125**(1–2): p. 111-119.
49. Han, Y., et al., *Molybdenum oxide modified HZSM-5 catalyst: Surface acidity and catalytic performance for the dehydration of aqueous ethanol.* Applied Catalysis A: General, 2011. **396**(1–2): p. 8-13.

50. Bian, G.-z., et al., *High temperature calcined K–MoO3/γ-Al2O3 catalysts for mixed alcohols synthesis from syngas: Effects of Mo loadings.* Applied Catalysis A: General, 1998. **170**(2): p. 255-268.
51. Pansanga, K., et al., *Effect of mixed γ- and χ-crystalline phases in nanocrystalline Al2O3 on the dispersion of cobalt on Al2O3.* Catalysis Communications, 2008. **9**(2): p. 207-212.
52. Khom-in, J., et al., *Dehydration of methanol to dimethyl ether over nanocrystalline Al2O3 with mixed γ- and χ-crystalline phases.* Catalysis Communications, 2008. **9**(10): p. 1955-1958.
53. Chakraborty, A. and B. Sun, *An adsorption isotherm equation for multi-types adsorption with thermodynamic correctness.* Applied Thermal Engineering, 2014. **72**(2): p. 190-199.
54. Radovic, L.R., *Chemistry & Physics of Carbon*. Vol. 29. 2004: CRC Press.
55. Inmanee, T., *Ethanol Dehydration reation over mixed phase Alumina catalysts*, 2013: Chulalongkorn University.
56. Wang, F., et al., *Corrigendum to "Coking behavior of a submicron MFI catalyst during ethanol dehydration to ethylene in a pilot-scale fixed-bed reactor" [Appl. Catal. A: Gen. 393 (2011) 161–170]*. Applied Catalysis A: General, 2011. **398**(1–2): p. 195.
57. Wang, C., et al., *Coking and deactivation of a mesoporous Ni–CaO–ZrO2 catalyst in dry reforming of methane: A study under different feeding compositions.* Fuel, 2015. **143**(0): p. 527-535.
58. Bail, A., et al., *Investigation of a molybdenum-containing silica catalyst synthesized by the sol–gel process in heterogeneous catalytic esterification reactions using methanol and ethanol.* Applied Catalysis B: Environmental, 2013. **130–131**(0): p. 314-324.
59. Shinohara, Y., et al., *Study of the interaction of ethanol with the Bronsted and Lewis acid sites on metal oxide surfaces using the DV-Xa method.* Journal of chemical software, 1997. **4**(41): p. 1-12.

APPENDIX

APPENDIX A
CONVERSION AND SELECTIVITY

Calculation of molybdenum oxide loading

The modified MoO_3 of alumina catalysts was prepared via impregnation of mixed phase alumina with an ammonium heptamolybdate tetrahydrate (AHM) solution. The preparation catalyst was calculated based on 1 gram of M-Al catalyst as below.

Based on 1 gram of M-Al catalyst was dropped 5wt.% of Mo. Thus the catalyst composition consists of:

Molybdenum = 0.05 gram

M-Al = 1.00-0.05 = 0.95 gram

Molybdenum 0.05 g. was prepared from ammonium heptamolybdate tetrahydrate ($(NH_4)_6Mo_7O_{24}\cdot 4H_2O$).

$$\text{AHM required} = \frac{\text{MW of } (NH_4)_6Mo_7O_{24}\cdot 4H_2O \times \text{Molybdenum required}}{\text{MW .of molybdenum}}$$

Where: - Molecular weight of $(NH_4)_6Mo_7O_{24}\cdot 4H_2O$ = 1,235.86 g/mol.

- Molybdenum (Mo), atomic weight = 95.96 g/mol.

Therefore, the AHM required was calculated follow formula as below

$$\text{AHM required} = \frac{1{,}235.86 \times 0.05}{95.96 \times 7} = 0.092 \text{ gram in } 0.95 \text{ gram}$$

$$\therefore \text{ AHM required on 1 g. of M-Al catalyst} = \frac{0.092 \times 1}{0.095}$$

$$= 0.0968 \text{ gram} \quad \underline{\text{Ans}}$$

APPENDIX B
CALIBRATION CURVE

Appendix B showed the calibration curves for calculation of composition of reactant and products in ethanol dehydration reaction as shown in **Figures B.1-B.4**. The reactant is ethanol and the main product is ethylene. The other products are DEE and acetaldehyde.

The concentration of reactant and products were analyzed by the gas chromatography Shimadzu model 14A, capillary column DB-5 of flame ionization detector (FID). The used conditions in GC are presented in **Table B.1**.

Table B. 1 Conditions use in GC-14A

Parameters	Condition
Width	5
Slope	100
Drift	0
Min. area	300
T.DBL	1000
Stop time	12 min.
Atten	2
Speed	3
Method	Normalization
SPL.WT	100
IS.WT	1

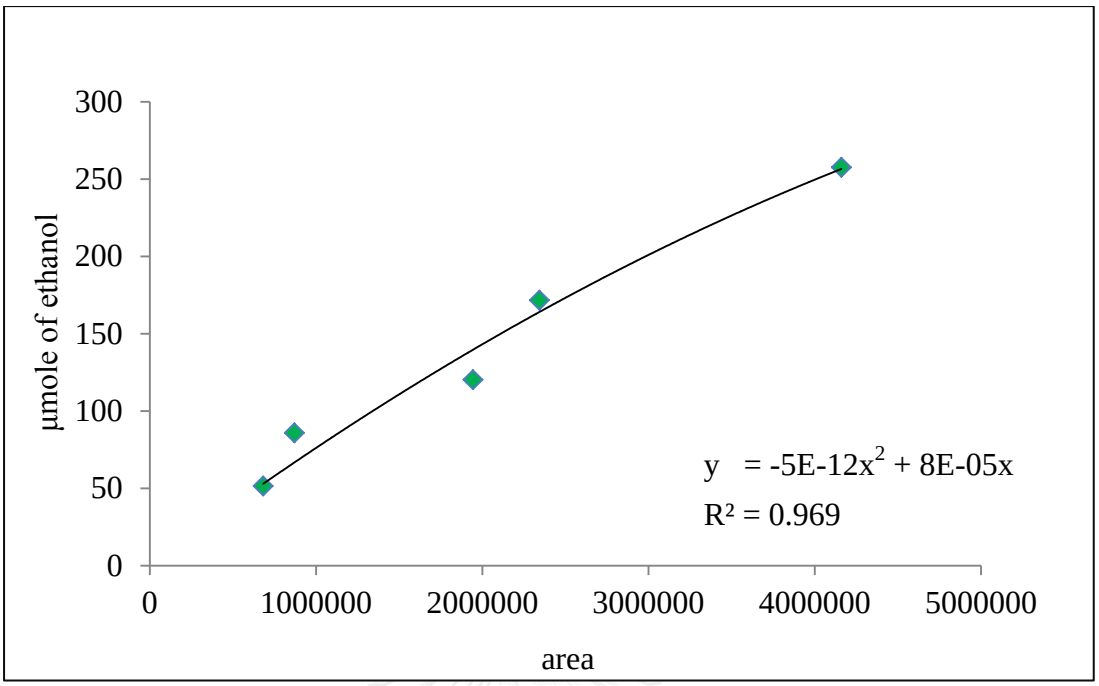

Figure B. 1 The calibration curve of ethanol

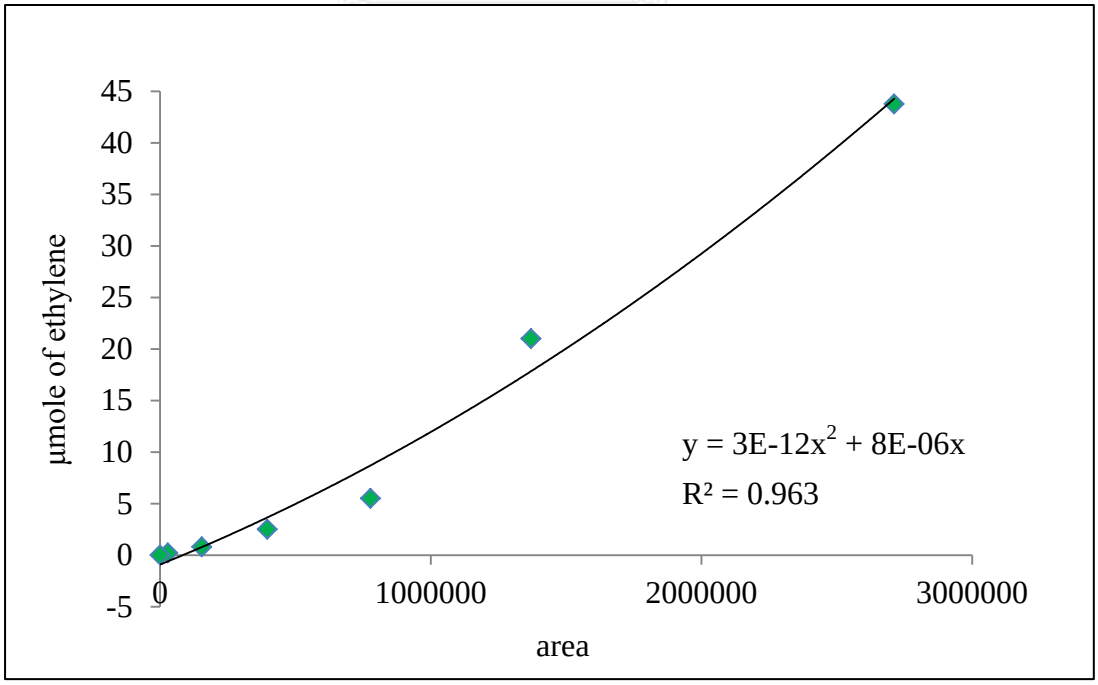

Figure B. 2 The calibration curve of ethylene

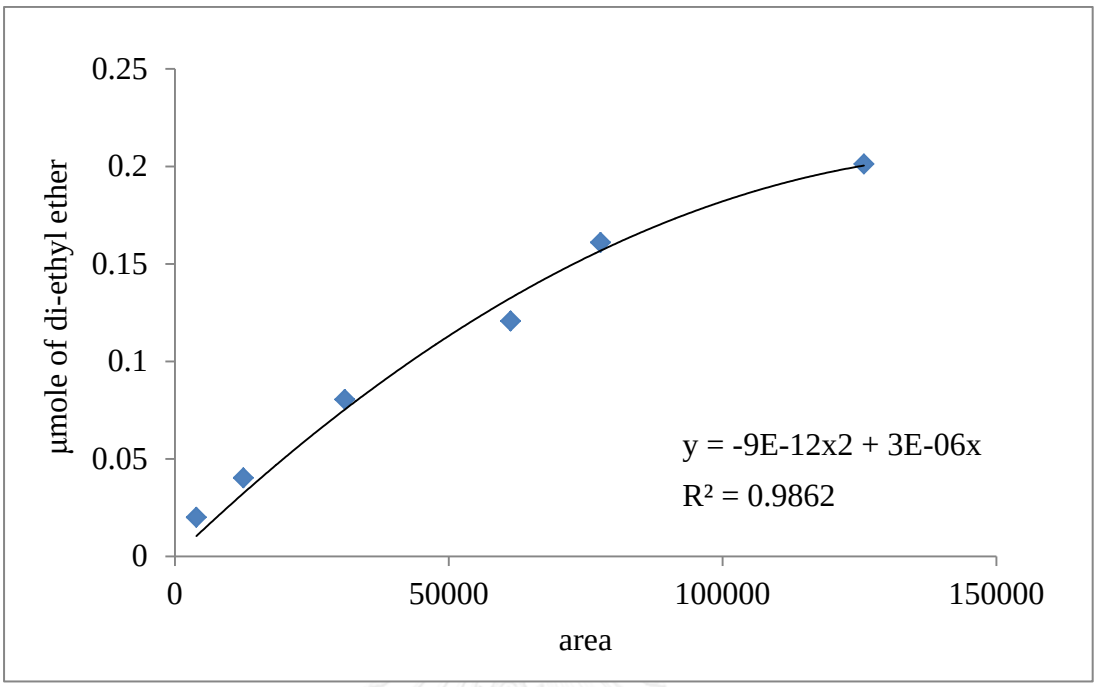

Figure B. 3 The calibration curve of DEE

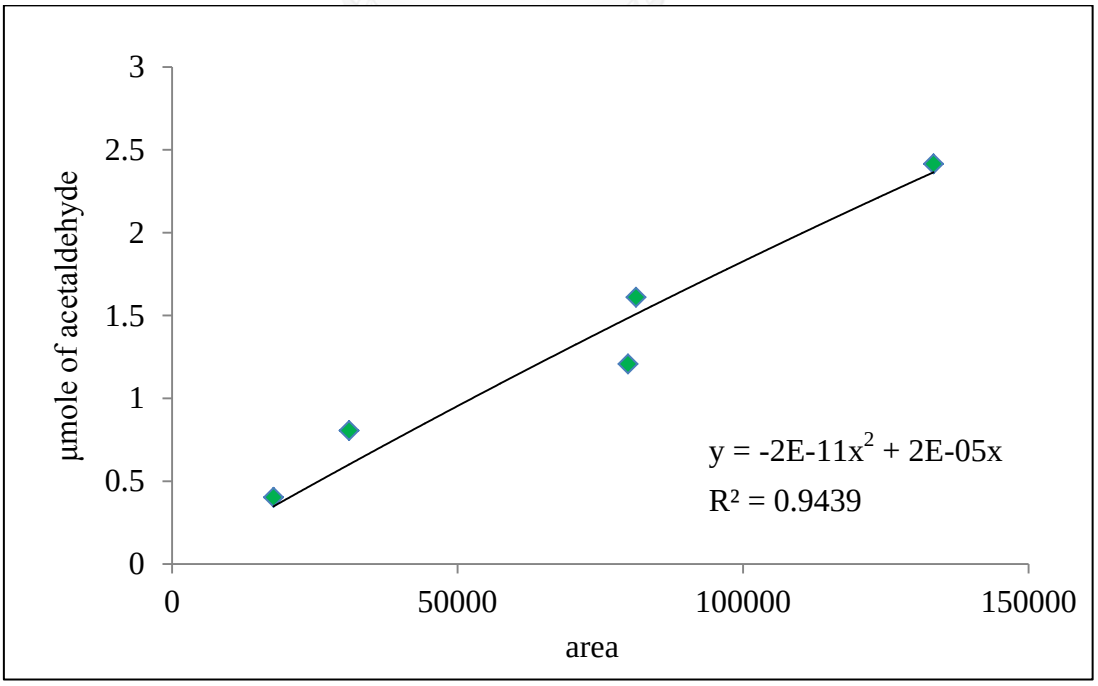

Figure B. 4 The calibration curve of acetaldehyde

APPENDIX C
CALCULATION OF CONVERSION AND SELECTIVITY

The catalyst performance for the ethanol dehydration was considered in term of ethanol conversion and selectivity of products.

Ethanol conversion is defined as usual:

$$\text{Conversion (\%)} = \frac{\text{Moles of reacted ethanol}}{\text{Moles of fed ethanol}} \times 100$$

While selectivity to product i is defined as follows:

$$\text{Selectivity (\%)} = \frac{\text{Moles of each product}}{\text{Total moles of the products}} \times 100$$

where: - Moles of each product (n_i) is the mole number of compound i (ethylene or DEE or acetaldehyde)

- Total moles products are ethylene, DEE, acetaldehyde; neglect another component (very low)

Moreover, the product yield was calculated as follows:

$$\text{Yield of i (\%)} = \text{Ethanol conversion} \times \text{Selectivity of i} \times 100$$

APPENDIX D
CALCULATION OF ACIDITY

The amount of acid site was represented for acidity of catalyst. In this research, the acidity was measured by NH_3-TPD technique, which amount of TCD signal versus temperature as follows:

$$\text{Amount of catalyst} = \frac{A}{\text{Amount of dry catalyst (g.)}}$$

where: - A is area under peak of NH_3-TPD profile × 0.0003 mole of NH_3 desorption based on calibration curve of micromeritics chemisorp 2750 Pulse Chemisorption System.

- The unit of amount of catalyst is mole of NH_3/g. cat.

APPENDIX E
CALCULATION OF REACTION RATE

Reaction rate

The ethanol dehydration occur several products from main and side reaction. There are investigated 3 products (ethylene, DEE, and acetaldehyde). The chemical reaction of each product is shown in equation E.1, E.2 and E.3 as follows:

Equation E.1

$C_2H_5OH \rightarrow C_2H_4 + H_2O$; $-r_{EtOH} = +r_E$

Equation E.2

$2\ C_2H_5OH \rightarrow C_4H_{10}O + H_2O$; $-\frac{1}{2}r_{EtOH} = +r_{DEE}$

Equation E.3

$C_2H_5OH \rightarrow C_2H_4O + H_2$; $-r_{EtOH} = +r_{AC}$

where: - r_{EtOH} = ethanol rate

- r_E = ethylene rate
- r_{DEE} = diethyl ether rate
- r_{AC} = acetaldehyde rate
- $r_{other\ components}$ = hydrocarbon, H_2, CO_2, etc. (side reaction)

Therefore, total rate of ethanol consumption can be rewritten as follows:

$$-r_{EtOH} = r_E + 2r_{DEE} + r_{AC} + r_{other\ components}$$

However, the reaction of substance was calculated as the following formula:

$$\text{Rate of component i} = \frac{\text{Concentration of component i} \times \text{Flow rate of EtOH}}{\text{Weight of catalyst}}$$

where: - The unit of rate of component i is μmol/hr.g.cat

- The unit of concentration of component i is μmol/ml
- Flow rate of EtOH is 1.45 ml/hr. (lab scale)
- Weight of catalyst uses 0.05 g.

The reaction rate was summarized in **Tables E.1-E.6**.

Table E. 1 Reaction rate of M-Al at temperature of 300°C

TOS	Product (μmol/ml)			Rate (μmol/hr.g.cat)			
(hrs.)	Ethylene	DEE	Acetaldehyde	Ethylene	DEE	Acetaldehyde	Ethanol
1	1.53	1.15	0.03	44.33	33.34	0.97	930.44
2	1.54	1.46	0.03	44.52	42.34	0.80	1015.86
3	1.52	1.06	0.02	44.18	30.74	0.49	1397.73
4	1.64	1.12	0.02	47.67	32.37	0.67	1542.09
5	1.69	0.76	0.05	48.95	22.09	1.33	1368.46
6	1.66	0.96	0.02	48.05	27.95	0.59	1358.06
7	1.34	0.75	0.03	38.85	21.76	0.77	1471.47
8	1.06	0.46	0.03	30.69	13.33	0.80	1485.57
9	1.31	0.92	0.02	38.12	26.67	0.60	1455.59
10	1.34	1.05	0.02	38.79	30.53	0.63	1382.34
11	1.32	0.70	0.03	38.31	20.37	0.84	1537.97
12	1.27	0.67	0.02	36.90	19.54	0.71	1461.33

Table E. 2 Reaction rate of M-Al at temperature of 350°C

TOS	Product (μmol/ml)			Rate (μmol/hr.g.cat)			
(hrs.)	Ethylene	DEE	Acetaldehyde	Ethylene	DEE	Acetaldehyde	Ethanol
1	4.34	0.27	0.13	125.74	7.91	3.85	635.65
2	4.79	0.25	0.16	138.99	7.21	4.61	871.43
3	5.58	0.35	0.15	161.89	10.15	4.46	866.88
4	5.05	0.25	0.17	146.33	7.15	4.96	839.84
5	5.36	0.28	0.15	155.47	8.22	4.21	892.97
6	5.30	0.27	0.15	153.75	7.81	4.45	900.00
7	4.68	0.20	0.16	135.69	5.91	4.60	870.93
8	4.70	0.16	0.17	136.40	4.58	4.79	906.08
9	5.00	0.19	0.15	144.94	5.39	4.35	902.60
10	5.79	0.17	0.19	167.95	4.85	5.50	914.23
11	5.87	0.19	0.19	170.13	5.61	5.47	916.47
12	4.88	0.12	0.14	141.57	3.41	4.08	923.46

Table E. 3 Reaction rate of M-Al at temperature of 400°C

TOS	Product (μmol/ml)			Rate (μmol/hr.g.cat)			
(hrs.)	Ethylene	DEE	Acetaldehyde	Ethylene	DEE	Acetaldehyde	Ethanol
1	7.10	0.09	0.11	205.99	2.56	3.07	582.65
2	5.75	0.07	0.08	166.81	1.99	2.36	891.31
3	5.98	0.08	0.08	173.47	2.22	2.27	917.36
4	6.03	0.06	0.08	174.82	1.72	2.31	929.04
5	5.68	0.06	0.08	164.75	1.84	2.20	969.24
6	6.84	0.08	0.09	198.43	2.35	2.56	985.04
7	5.82	0.00	0.11	168.66	0.06	3.12	1814.10
8	6.67	0.00	0.12	193.50	0.08	3.54	2079.52
9	7.17	0.01	0.14	208.04	0.20	3.93	2138.90
10	5.54	0.00	0.11	160.73	0.07	3.13	2167.45
11	4.72	0.00	0.06	136.75	0.03	1.80	2216.47
12	3.34	0.01	0.03	96.72	0.15	0.85	2285.42

Table E. 4 Reaction rate of Mo-M-Al at temperature of 300°C

TOS	Product (μmol/ml)			Rate (μmol/hr.g.cat)			
(hrs.)	Ethylene	DEE	Acetaldehyde	Ethylene	DEE	Acetaldehyde	Ethanol
1	1.07	1.08	0.17	30.97	31.24	4.81	368.60
2	1.13	1.17	0.16	32.65	33.93	4.67	500.78
3	1.14	1.04	0.16	32.94	30.12	4.74	545.80
4	1.17	1.07	0.16	33.85	31.12	4.70	556.02
5	1.18	1.06	0.15	34.16	30.75	4.32	587.22
6	1.20	1.06	0.15	34.74	30.65	4.29	603.18
7	1.06	0.94	0.11	30.70	27.22	3.26	375.94
8	1.07	1.05	0.12	31.09	30.41	3.41	419.91
9	1.14	1.23	0.13	33.15	35.66	3.78	405.02
10	1.13	0.94	0.13	32.81	27.31	3.78	475.74
11	1.12	0.96	0.13	32.43	27.90	3.73	578.75
12	1.14	1.26	0.12	32.97	36.49	3.49	461.27

Table E. 5 Reaction rate of Mo-M-Al at temperature of 350°C

TOS	Product (μmol/ml)			Rate (μmol/hr.g.cat)			
(hrs.)	Ethylene	DEE	Acetaldehyde	Ethylene	DEE	Acetaldehyde	Ethanol
1	3.20	0.78	0.58	92.89	22.63	16.96	499.53
2	0.05	0.00	0.01	1.49	0.08	0.42	957.89
3	2.62	0.37	0.55	75.88	10.61	15.82	827.39
4	2.65	0.38	0.49	76.92	11.07	14.17	842.99
5	3.08	0.47	0.49	89.19	13.64	14.33	827.20
6	3.30	0.52	0.50	95.68	15.00	14.62	805.88
7	2.28	0.51	0.44	66.15	14.73	12.70	567.79
8	3.31	0.95	0.55	96.10	27.44	15.98	609.24
9	2.66	0.45	0.46	77.00	13.19	13.34	755.55
10	2.58	0.51	0.48	74.85	14.73	13.92	773.59
11	2.71	0.54	0.51	78.45	15.73	14.68	724.86
12	2.56	0.56	0.49	74.24	16.18	14.07	733.85

Table E. 6 Reaction rate of Mo-M-Al at temperature of 400°C

TOS	Product (μmol/ml)			Rate (μmol/hr.g.cat)			
(hrs.)	Ethylene	DEE	Acetaldehyde	Ethylene	DEE	Acetaldehyde	Ethanol
1	4.59	0.03	0.58	132.99	0.89	16.87	504.64
2	6.28	0.03	0.71	182.00	0.78	20.49	887.80
3	6.35	0.02	0.72	184.22	0.48	20.95	933.48
4	5.26	0.01	0.51	152.46	0.27	14.86	954.07
5	5.05	0.01	0.44	146.58	0.28	12.74	959.02
6	5.81	0.08	0.77	168.44	2.45	22.28	915.69
7	3.47	0.01	0.28	100.75	0.18	8.10	1037.29
8	6.17	0.01	0.66	179.06	0.41	19.22	1026.26
9	7.16	0.05	0.64	207.51	1.55	18.55	1008.49
10	8.14	0.05	0.72	236.10	1.58	20.82	1013.44
11	7.17	0.05	0.60	207.96	1.56	17.36	1013.56
12	6.04	0.02	0.48	175.16	0.72	13.93	1025.98

APPENDIX F
LIST OF PUBLICATION

Proceeding

Jarurat Sumphawanich and Bunjerd jongsomjit, "Stability of mixed-phase alumina catalysts for ethanol dehydration reaction." Proceeding of the 3rd national interdisciplinary academic conference TNIAC 2015, Thai-Nichi Institute of Tecnology Bangkok, Thailand, May 15 2015.

VITA

Miss Jarurat Sumphanwanich was born on Jan 25th, 1989 in Bangkok province,Thailand. She graduated the bachelor’s degree in chemical engineering department, faculty of engineering, Kasetsart University (KU) in May 10, 2011. She continued to study master's degree in chemical engineering department, faculty of engineering, Chulalongkorn University (CU) in October 2012.